two macrophage-derived interferon-gamma-inducing factors (IL-12 and IL-15) induces a lethal systemic inflammatory response in mice that is dependent on natural killer cells but does not require interferon-gamma. Cell Immunol 216(1–2):31–42
35. Tsushima H, Ito N, Tamura S, Matsuda Y, Inada M, Yabuuchi I, Imai Y, Nagashima R, Misawa H, Takeda H, Matsuzawa Y, Kawata S (2001) Circulating transforming growth factor beta 1 as a predictor of liver metastasis after resection in colorectal cancer. Clin Cancer Res 7(5):1258–1262
36. Okumoto K, Hattori E, Tamura K, Kiso S, Watanabe H, Saito K, Saito T, Togashi H, Kawata S (2004) Possible contribution of circulating transforming growth factor-beta1 to immunity and prognosis in unresectable hepatocellular carcinoma. Liver Int 24(1):21–28
37. Chau GY, Wu CW, Lui WY, Chang TJ, Kao HL, Wu LH, King KL, Loong CC, Hsia CY, Chi CW (2000) Serum interleukin-10 but not interleukin-6 is related to clinical outcome in patients with resectable hepatocellular carcinoma. Ann Surg 231(4):552–558
38. Galizia G, Lieto E, De Vita F, Romano C, Orditura M, Castellano P, Imperatore V, Infusino S, Catalano G, Pignatelli C (2002) Circulating levels of interleukin-10 and interleukin-6 in gastric and colon cancer patients before and after surgery: relationship with radicality and outcome. J Interferon Cytokine Res 22(4):473–482
39. Meadows SK, Eriksson M, Barber A, Sentman CL (2006) Human NK cell IFN-gamma production is regulated by endogenous TGF-beta. Int Immunopharmacol 6(6):1020–1028
40. Caruso M, Pham-Nguyen K, Kwong YL, Xu B, Kosai KI, Finegold M, Woo SL, Chen SH (1996) Adenovirus-mediated interleukin-12 gene therapy for metastatic colon carcinoma. Proc Natl Acad Sci USA 93(21):11302–11306
41. Barajas M, Mazzolini G, Genove G, Bilbao R, Narvaiza I, Schmitz V, Sangro B, Melero I, Qian C, Prieto J (2001) Gene therapy of orthotopic hepatocellular carcinoma in rats using adenovirus coding for interleukin 12. Hepatology 33(1):52–61
42. Sangro B, Mazzolini G, Ruiz J, Herraiz M, Quiroga J, Herrero I, Benito A, Larrache J, Pueyo J, Subtil JC, Olague C, Sola J et al (2004) Phase I trial of intratumoral injection of an adenovirus encoding interleukin-12 for advanced digestive tumors. J Clin Oncol 22(8):1389–1397

ELSEVIER

Journal of Hepatology 50 (2009) 1155–1162

Journal of Hepatology

www.elsevier.com/locate/jhep

Activated liver dendritic cells generate strong acquired immunity in α-galactosylceramide treatment☆

Akira Sasakawa[1,2], Tomohide Tatsumi[1,2], Tetsuo Takehara[1,2], Shinjiro Yamaguchi[1,2], Masashi Yamamoto[1,2], Kazuyoshi Ohkawa[1], Takuya Miyagi[1], Norio Hayashi[1,2,*]

[1]*Department of Gastroenterology and Hepatology, Osaka University Graduate School of Medicine, 2-2 Yamadaoka, Suita, Osaka 565-0871, Japan*
[2]*Core Research for Evolutional Science and Technology (CREST), Japan Science and Technology Agency (JST), Tokyo, Japan*

***Background/Aims*: α-Galactosylceramide (α-GalCer) presented by dendritic cells (DCs) activates NKT cells that in turn drive DC maturation. However, the potential of generating acquired immunity of liver DCs in α-GalCer treatment remains unclear.**

***Methods*: We examined the activation of acquired immunity in the α-GalCer treatment against liver or spleen tumor and the ability of liver and spleen DCs in the generation of acquired immunity.**

***Results*: Administration of α-GalCer resulted in generation of p53 peptide-specific cytotoxic T lymphocytes (CTLs) in mice bearing liver CMS4 tumor, aberrantly expressing p53, but not in mice bearing spleen CMS4 tumor. The growth of rechallenged CMS4 subcutaneous tumor was inhibited in α-GalCer-treated mice against liver CMS4 tumor, but not in α-GalCer-treated mice against CMS4 spleen tumor. The antigen presenting related functions of liver DCs were significantly higher than those of spleen DCs in α-GalCer-treated mice. Vaccination of normal mice with p53 peptide pulsed liver DCs isolated from α-GalCer treated mice resulted in generation of p53 peptide-specific CTLs, but that with p53 peptide pulsed spleen DCs did not.**

***Conclusions*: These results demonstrated that α-GalCer treatment induced unique immunologic activation of liver DCs in comparison with spleen DCs, which might be favorable to generate liver acquired immunity.**

***Keywords*: α-Galactosylceramide; Liver dendritic cells; Acquired antitumor immunity**

1. Introduction

α-Galactosylceramide (α-GalCer) presented by CD1d molecules expressing on dendritic cells (DCs) efficiently stimulates NKT cells implicated in innate immunity [1,2]. Recently, *in vivo* animal studies have shown that systemic administration of α-GalCer can lead to anti-tumor effects against metastatic liver tumor [3,4], suggesting that α-GalCer treatment might be promising for clinical application against liver tumor. Metastatic liver tumors resist conventional chemotherapy and radiotherapy, and present with a poor prognosis. Thus novel and more effective immunotherapy is needed, especially for metastatic liver cancer. Several phase I clinical studies have been done in cancer immunotherapy using intravenous administration of α-GalCer, but with limited clinical responses [5,6]. For further development of α-GalCer treatment in liver cancer patients, the antitumor effect of α-GalCer should be more precisely examined in the liver.

DCs effectively elicit immune responses to self and foreign antigens [7,8]. These specialized antigen-presenting cells (APCs) can induce the generation of both

Received 9 September 2008; received in revised form 9 December 2008; accepted 13 December 2008; available online 26 February 2009
Associate Editor: V. Barnaba

☆ The authors declare that they do not have anything to disclose regarding funding from industries or conflict of interest with respect to this manuscript.

* Corresponding author. Fax: +81 6 68793629.
E-mail address: hayashin@gh.med.osaka-u.ac.jp (N. Hayashi).

Abbreviations: DC, dendritic cell; APC, antigen-presenting cells; CTLs, cytotoxic T lymphocytes; α-GalCer, α-galactosylceramide; MNC, mononuclear cells.

0168-8278/$36.00 © 2009 Published by Elsevier B.V. on behalf of the European Association for the Study of the Liver.
doi:10.1016/j.jhep.2008.12.027

antigen-specific cytotoxic T lymphocytes (CTLs) and T helper cells. α-GalCer administration resulted in maturation of spleen DCs and activation of the CD8+ T cell immune response via costimulatory molecules expressed on the spleen DCs [9,10]. However, in contrast to well-characterized spleen DCs, the details of activation of liver DCs by α-GalCer treatment remains to be clarified because of the difficulty of procuring adequate numbers of isolated liver DCs for functional analysis [11]. Although most previous studies reported that α-GalCer treatment induces early activation of liver NKT and NK cells [3,4,12], which were the main effector cells to eradicate metastatic tumor cells, little is known regarding the induction of liver acquired immunity after early rejection of liver tumor. Nakagawa et al. reported that CD122+CD8+ memory T cells play critical roles in metastatic liver tumor rejection by α-GalCer treatment [13]. However, the ability of α-GalCer to activate liver DCs and generate acquired immunity remains to be clarified.

In the current study, we evaluated the induction of acquired immunity by α-GalCer activated liver DCs in comparison with spleen DCs. We demonstrated that α-GalCer treatment resulted in generating strong acquired immunity after liver tumor treatment, but not after spleen tumor treatment. We also show that α-GalCer treatment activated liver DCs more strongly with respect to the antigen-presenting function and antigen-specific CTL induction than spleen DCs. Thus, α-GalCer treatment resulted in unique immunologic activation of liver DCs, which might contribute to induction of acquired immunity in the liver.

2. Materials and methods

2.1. Mice and cell lines

Six-to-ten-week-old female BALB/c mice and C57BL/6 mice were purchased from Shizuoka Experimental Animal Laboratory (Shizuoka, Japan). The animals were handled under aseptic conditions. Procedures were performed according to approved protocols and in accordance with recommendations for the proper care and use of laboratory animals. CMS4 sarcomas (H-2^d) express mutated p53 and present the wild-type $p53_{232-240}$ epitope recognized by H-$2K^d$-restricted CTLs [14,15], and MC38 colon cancer cell lines were maintained as previously described [16]. α-Galactosylceramide (α-GalCer) was kindly provided by Kirin Pharma (Gunma, Japan) and prepared as previously described [15].

2.2. IFN-γ ELISPOT assays for p53 peptide-reactive CD8+ T cells responses after α-GalCer treatment for CMS4 tumor and animal experiments

To examine the induction of the acquired antitumor immunity, BALB/c mice were injected intrahepatically or intrasplenically with 5×10^5 CMS4 cells on day 0 and treated intraperitoneally (i.p.) with α-GalCer (2 μg/100 μl) or 100 μl of vehicle on day 1. Fourteen days after α-GalCer treatment, CD8+ T cells were isolated from the spleen of immunized mice by using magnetic beads (MACS, Miltenyi Biotec, Gladbach, Germany). Next, CD8+ T cells (1×10^5 cells/well) and syngeneic bone marrow derived DCs (BMDCs) generated from normal BALB/c mice (2×10^4 cells/well) were cocultured with $p53_{232-240}$ peptide in ELISPOT culture plate. We used mouse IFN-γ ELISPOT kit (R & D Systems, Minneapolis, MN) to detect the $p53_{232-240}$ peptide-specific CD8+ T cell responses, as previously described [16]. To assess the systemic acquired immunity due to α-GalCer treatment, mice were injected in the liver or the spleen with 5×10^5 CMS4 cells or MC38 cells on day 0 and were injected i.p. with α-GalCer on day 1. On day 14 after α-GalCer treatment, 1×10^6 CMS4 cells or MC38 cells were injected as a rechallenge into the right flank of treated mice, respectively. Tumor size was assessed every 7 days.

2.3. Preparation of liver and spleen DCs and flow cytometry

Twenty-four hours after i.p. treatment with α-GalCer or vehicle, hepatic mononuclear cells (MNC) and splenic MNC were prepared as previously described [15]. CD11c+ dendritic cells were isolated from liver MNC and spleen MNC by magnetic cell sorting using MACS (Miltenyi Biotec) according to the manufacturer's protocol. For phenotypic analysis of liver and spleen DCs, PE- or FITC- or APC-conjugated monoclonal antibodies against mouse cell surface molecules [CD11c (Miltenyi Biotec), CD40, CD80, CD86, MHC class II, CD8α and CD11b (all from BD-Pharmingen, San Diego, CA)] were used, and flow cytometric analysis was performed using a FACS Calibur (Becton Dickinson, San Jose, CA) flow cytometer. We defined DCs with CD11c+ MHC class II+ cells by flow cytometry and evaluated the expressions of these antigen presenting related molecules. Data were analyzed using FlowJo software (Tree Star, Ashland, OR) and reported as the mean fluorescence intensity (MFI).

2.4. Cytokine measurement

Twenty-four hours after i.p. treatment with α-GalCer or vehicle, liver and spleen DCs were prepared as above. To assess cytokine production, we cultured 2×10^5 DCs in 1 ml of complete medium with LPS (R & D Systems Inc., 10 μg). After 48 h, cell culture supernatants were harvested and tested using a species-specific enzyme linked immunosorbent assay (ELISA) kit for IL-12, IFN-γ and TNF-α (BD-Pharmingen) according to the manufacturer's protocols.

2.5. T cell proliferation assay

Twenty-four hours after i.p. treatment with α-GalCer or vehicle, liver and spleen DCs were prepared as above. The DCs were added in various numbers to 5×10^5 allogeneic T lymphocytes (purified using Thy-1.2 immunomagnetic microbeads from C57BL/6 mice) in 96-well U-bottom plates and then pulsed with [^{3}H] thymidine (1 μ Ci/well) on day 3 for an additional 20 h as previously described [17].

2.6. Immunization of p53 peptide-pulsed liver or spleen DCs from α-GalCer-treated mice

Twenty-four hours after i.p. treatment with α-GalCer or vehicle, liver and spleen DCs were prepared as above. Isolated DCs were incubated with $p53_{232-240}$ peptide at concentration of 10 μg/mL per 10^6 DCs/mL for 2 h as previously described [14]. 1×10^6 $p53_{232-240}$ peptide pulsed liver or spleen DCs were injected i.p. into normal BALB/c mice. Five days after i.p. immunization, CD8+ T cells were isolated from the spleen of immunized mice by using magnetic beads (MACS) and were subjected to mouse IFN-γ ELISPOT assay as above described.

2.7. Statistical analyses

The statistical significance of differences between the groups was determined by applying Student's *t*-test with Welch correction after each group had been tested with equal variance and Fisher exact probability test. The statistical significance of the differences in more than three groups was determined by applying one-way ANOVA. Statistical significance was defined as $p < 0.05$.

3. Results

3.1. Acquired antitumor immunity was induced by α-GalCer treatment of CMS4 liver tumor

We examined whether α-GalCer treatment for CMS4 liver or spleen tumor would induce acquired antitumor immunity. Mice bearing liver or spleen CMS4 tumor were treated i.p. with α-GalCer. Fourteen days after α-GalCer treatment, spleen CD8+ T cells from treated mice were prepared and subjected to IFN-γ ELISPOT. The high numbers of IFN-γ spots were detected in the CMS4 liver tumor model, but not in the CMS4 spleen tumor model (Fig. 1A).

We next analyzed whether the α-GalCer treatment of CMS4-treated liver or spleen would impact the progression of subcutaneous rechallenged CMS4 tumors. Fourteen days later after α-GalCer treatment, 1×10^6 CMS4 cells were rechallenged subcutaneously in the right flank. As shown in Fig. 1B, CMS4 subcutaneous tumors in α-GalCer treated mice bearing CMS4 liver tumor were significantly inhibited compared with those in non-treated mice, but those in mice bearing CMS4 spleen tumor were not. Colon26, BALB/c syngeneic colon cancer cell, subcutaneous tumors were not inhibited in mice receiving α-GalCer treatment for CMS4 liver or spleen tumor (data not shown). Strong acquired immunity could also be generated after α-GalCer treatment of MC38 liver tumors in C57BL/6 mice, but not of MC38 spleen tumors (Fig. 1C). These findings suggested that tumor-specific acquired immunity could be generated efficiently by α-GalCer treatment in the liver, but not in the spleen.

3.2. Administration of α-GalCer activated DCs and increased CD8- conventional DC fraction in the liver

Recent research revealed that NKT cells-DC interactions by α-GalCer are critically important in the sequential activation of effector cells in both innate and acquired immunity [12,18]. However, details of the DC activation by α-GalCer in the liver have not yet been evaluated.

First, we investigated the increase of liver and spleen DCs after α-GalCer or vehicle treatment. As shown in Fig. 2A, liver DCs increased significantly after α-GalCer administration whereas spleen DCs from α-GalCer treated mice did not. The proportion of liver DCs in liver MNCs also significantly increased by α-GalCer administration, but that of spleen DCs did not (data not shown). Next, we examined the change of DC subtypes after α-GalCer treatment by analyzing the relative surface expressions of the CD8α and the CD11b molecules [19]. The proportion and the number of CD8- conventional DCs (CD11b+CD8-) significantly increased in the liver by α-GalCer treatment, but not in the spleen. In marked contrast, those of CD8+ conventional DCs (CD11b-CD8α+) exhibited no significant change in both the liver and spleen by α-GalCer treatment (Fig. 2B and C).

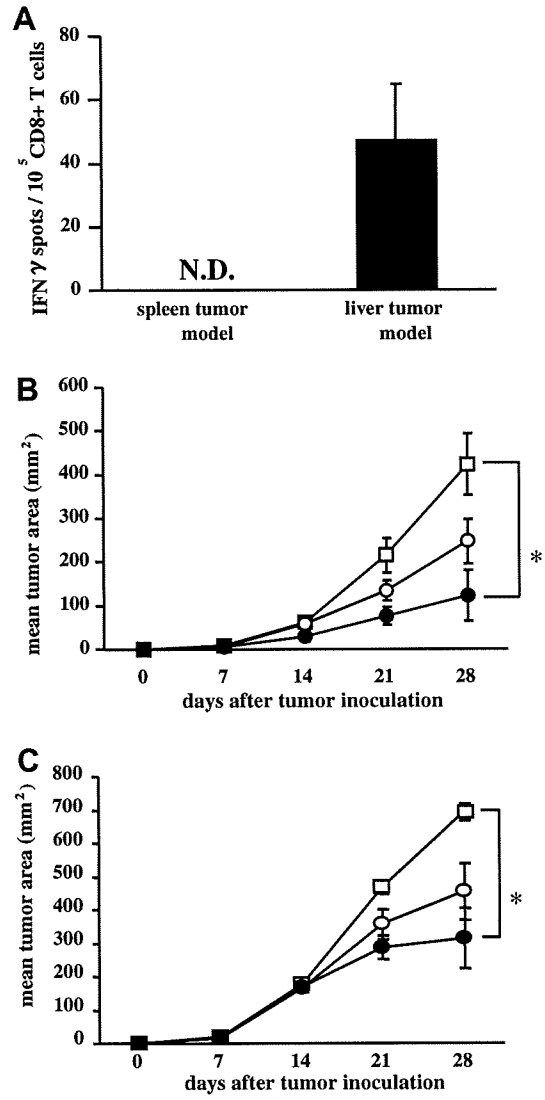

Fig. 1. Induction of local and systemic acquired antitumor immunity after α-GalCer treatment of CMS4 liver and spleen tumor. BALB/c mice were injected intrahepatically or intrasplenically with 5×10^5 CMS4 cells or MC38 cells. One day later, mice were injected i.p. with α-GarCer. (A) Fourteen days later, spleen CD8+ T cells were isolated from both the CMS4 liver and spleen tumor models and subjected to IFN-γ ELISPOT to analyze $p53_{232-240}$ peptide specific IFN-γ production. The results are shown as spots/100,0000 CD8+ T cells; mean ± SD of triplicate samples. CD8+ T cell reactivity against peptide-unpulsed BMDCs served as the negative control in all cases, and this value was subtracted from all experimental determination to determine p53-specific spot numbers. $^*p < 0.05$. N.D., not detected. Similar results were obtained from two separate experiments. (B and C) Fourteen days later, mice were challenged subcutaneously with 1×10^6 CMS4 cells (B) or MC38 cells (C) in the right flank (all treatment groups $N = 8$). Tumor size was assessed every 7 days after subcutaneous injection of tumor cells (=on day 0). α-GalCer-treated CMS4 or MC38 liver tumor (•), α-GalCer-treated CMS4 or MC38 spleen tumor (○), non-treated mice (□). Each data point represents the mean tumor size ±SE. $^*p < 0.05$.

We examined the CD80, CD86 and CD40 expressions of liver and spleen DCs after administration of α-GalCer. CD86 and CD40 molecules on both liver and spleen DCs from α-GalCer-treated mice were

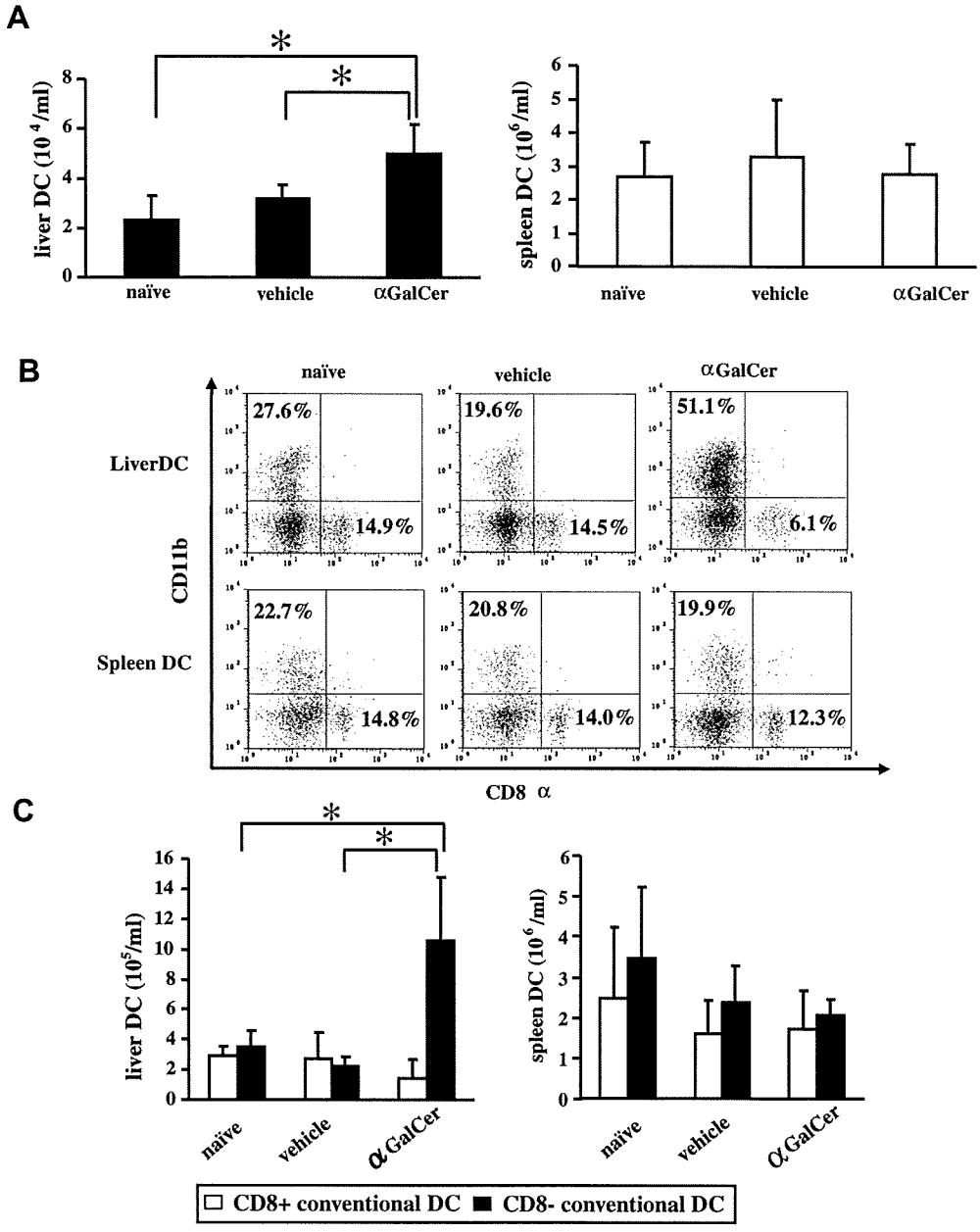

Fig. 2. α-GalCer treatment increased liver CD8- conventional DC. BALB/c mice were treated with α-GalCer or vehicle. Liver and spleen DCs were prepared on day 1 after α-GalCer treatment. (A) Liver DCs (left panel) increased significantly after α-GalCer treatment, but spleen DCs (right panel) did not. (B and C) The change of CD8+ or CD8- conventional DC subtypes after α-GalCer treatment was examined by flow cytometry. The data are represented as the average of numbers obtained from 5 separate experiments. $^*p < 0.05$.

expressed more strongly than those from vehicle-treated mice and non-treated mice. CD80 molecules on liver DC from α-GalCer-treated mice were expressed significantly more strongly than those from vehicle-treated or non-treated mice, but those on spleen DC showed no significant change by α-GalCer treatment (Fig. 3). The expressions of CD80, CD86 and CD40 molecules on liver DCs tended to be lower than those on spleen DCs in non-treated mice. However, after α-GalCer treatment, their expressions on liver DCs tended to increase to levels similar to those on spleen DCs.

3.3. Liver DCs from α-GalCer-treated mice could produce more Th1 cytokines and present higher T cell immunostimulatory ability than spleen DCs

Th1-cytokines, such as IL-12, INF-γ and TNF-α, play key roles in determining the strength and/or the phenotypes of the antitumor immune responses [20,21]. We next examined the production of Th1 cytokines from DCs after α-GalCer treatment. The production of these cytokines from DCs derived from vehicle-treated and non-treated mice were not detected in the

liver or the spleen. In marked contrast, all IL-12, INF-γ and TNF-α production from liver DCs derived from α-GalCer-treated mice were significantly higher than those from spleen DCs (Fig. 4A–C). To investigate the difference of the antigen-presenting function between liver DCs and spleen DCs, we examined the allostimulatory capacity of liver and spleen DCs using a mixed lymphocyte reaction (MLR). Liver DCs from α-GalCer-treated mice showed higher T cell proliferation ability than those from vehicle-treated or non-treated mice and spleen DCs from all treatment groups. Spleen DCs from all treatment groups and liver DCs from vehicle-treated or non-treated mice showed little T cell proliferation ability (Fig. 4D). These results suggested that α-GalCer treatment increased the function of DCs in the liver more strongly than those in the spleen.

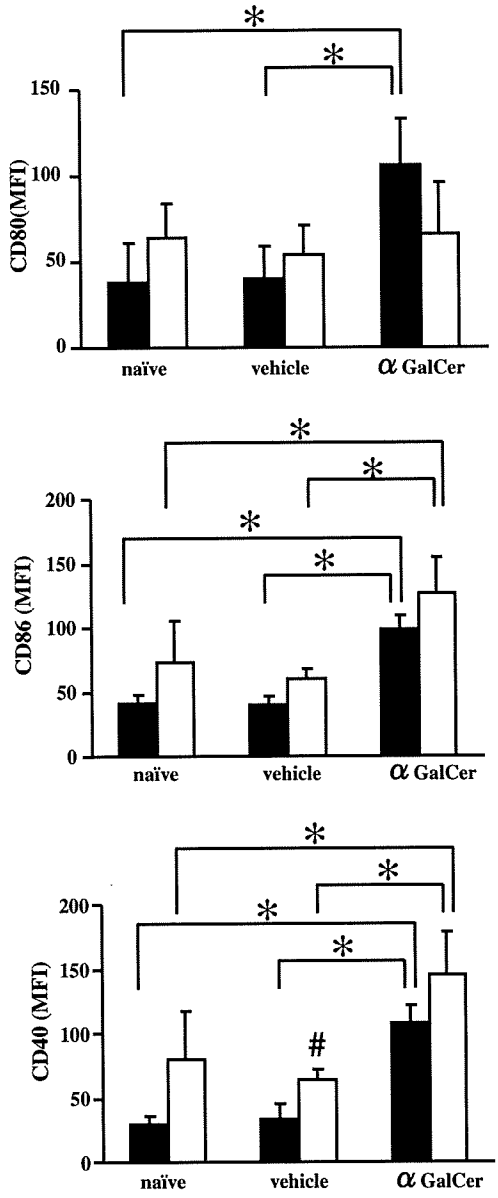

Fig. 3. α-GalCer treatment increased the expression of antigen presenting related molecules on both liver and spleen DCs. DCs were stained with PE- or FITC-conjugated monoclonal antibodies (CD11c, CD40, CD80, CD86 and MHC class II), and the expressions of these molecules were analyzed by flow cytometry. The data are represented as the average of MFI obtained from 5 separate experiments. $^{*}p < 0.05$ for each treatment group, $^{\#}p < 0.05$ between liver DCs (■ black bar) and spleen DCs (□ white bar). Naïve: DCs derived from non-treated mice; vehicle: DCs derived from vehicle-treated mice; α-GalCer: DCs derived from α-GalCer-treated mice.

3.4. Vaccination of $p53_{232-240}$ peptide-pulsed liver DCs isolated from α-GalCer-treated mice resulted in generating $p53_{232-240}$ peptide specific CTLs more efficiently than that of spleen DCs

Based on the above results, liver DCs had more antigen-presenting function than spleen DCs in α-GalCer-treated mice. We next evaluated the potential of tumor associated antigen specific CTL induction by vaccination of peptide-pulsed liver DCs or spleen DCs. We vaccinated normal mice i.p. with peptide-pulsed DC. Five days later, spleen CD8+ T cells were isolated and subjected to IFN-γ ELISPOT assay. As shown in Fig. 5, the numbers of IFN-γ spots observed for T cell responses against $p53_{232-240}$ peptide in mice vaccinated with α-GalCer-activated liver DCs were significantly higher than those in mice with vehicle- or non-treated-liver DCs. There were no detectable spots in mice vaccinated with spleen DCs from all treatment groups, suggesting that spleen DCs displayed no stimulatory activity for CTL induction regardless of the administration of α-GalCer *in vivo*. These results revealed that liver DCs in α-GalCer-treated mice have the highest potential for inducing tumor-associated antigen-specific CTLs, which might be associated with the *in vivo* generation of acquired immunity against liver tumor by α-GalCer treatment shown in Fig. 1.

4. Discussion

We and others previously reported that the early eradication of tumor cells in the liver mainly depended on NKT cells and NK cells [3,4]. In this study, we demonstrated that α-GalCer treatment resulted in generating stronger acquired immunity after eradication of primary CMS4 and MC38 liver tumor, but not after spleen tumor treatment. This suggests that liver, and not spleen, is an unique immunological organ that is favorable for generation of acquired immunity. We examined whether CTLs generated by immunization with peptide- and α-GalCer-pulsed BMDC could show equally antitumor effect in skin, liver and spleen in the normal mice. The generated CTLs in treated mice have equal access to all organs and are capable of killing tumor cells (Sasakawa, unpublished data). Thus, our data encour-

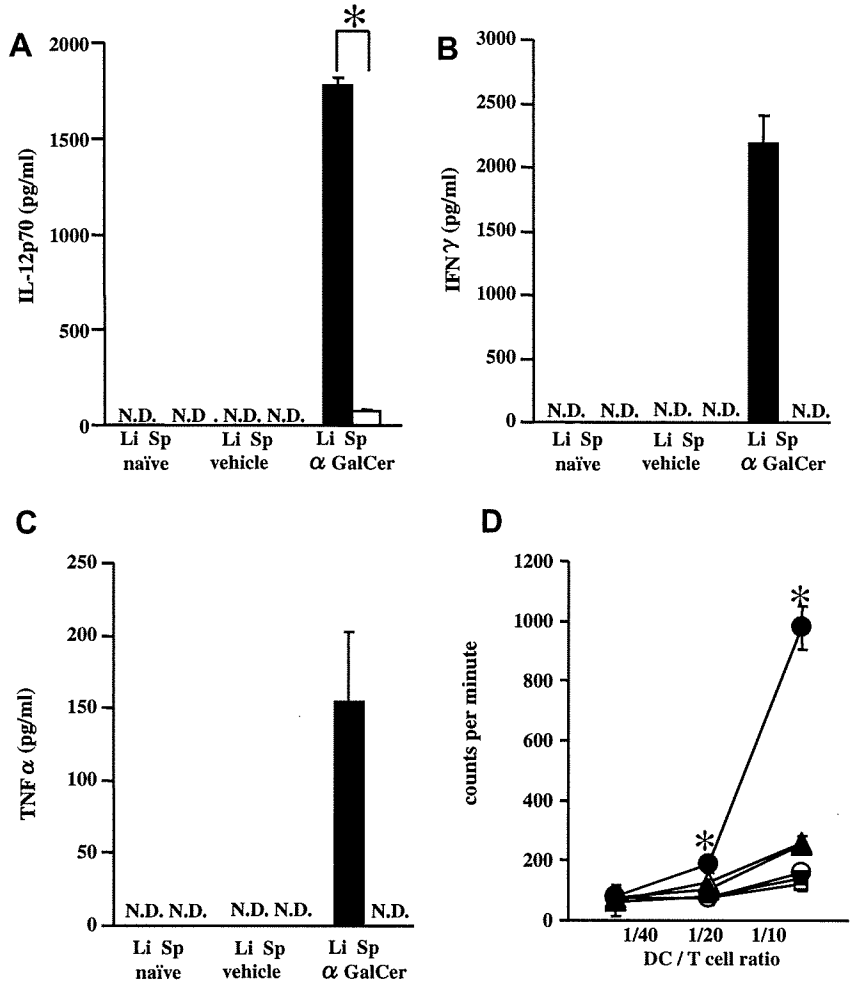

Fig. 4. Th1 type cytokine production of liver DCs from α-GalCer treated mice. Liver and spleen DCs were prepared 24 h after i.p. treatment of α-GalCer or vehicle. 2×10^5 DCs were stimulated with LPS (10 μg), and the supernatants of the DC cultures were subjected to specific ELISA. IL-12 (A), IFN-γ (B) and TNF-α (C). N.D., not detected. (D) We examined the allostimulatory capacity of liver and spleen DCs by MLR. Liver DC from non-treated mice (■), vehicle-treated mice (▲), and α-GalCer-treated mice (●). Spleen DC from non-treated mice (□), vehicle-treated mice (△), and α-GalCer-treated mice (○). Each data point represents the mean tumor size ± SD. $^*p < 0.05$ counts per minute (CPM) of liver DCs vs CPM of spleen DCs from α-GalCer, vehicle or non-treated mice, respectively. Similar results were obtained from three separate experiments.

aged us to investigate the ability of liver DC to generate acquired antitumor immunity in comparison with spleen DCs.

In the current study, we investigated the activation of liver and spleen DC function after α-GalCer treatment. The expressions of antigen-presenting related molecules on liver DCs were weaker than those on spleen DCs in normal or vehicle treated mice. Pillarisetty et al. reported that liver DCs are generally weak activators of immunity in contrast to spleen DCs in normal mice and the expressions of MHC and costimulatory molecules on liver DCs were lower than those on spleen DCs in normal mice [22]. This is consistent with our results. In marked contrast, α-GalCer administration resulted in a significant increase of DCs in the liver and the expressions of antigen-presenting related molecules was more strongly upregulated in the liver than in the spleen. It has been reported that the expression of CD8α molecule is an activating marker of conventional DCs from progenitor cells [23]. We demonstrated that α-GalCer administration induced not only an increase of total DCs but also a significant increase of CD8- conventional DCs in the liver, which suggested that α-GalCer treatment resulted in developing progenitor DCs efficiently to matured conventional DCs. More strikingly, the production of Th1 type cytokine from α-GalCer-treated liver DCs were significantly more than from α-GalCer-treated spleen DCs. Previous reports demonstrated that the capacity of Th1 type cytokine to link between innate and adaptive immunity by interacting with DCs and T cells, is important for the induction of adaptive antitumor immune response and long-term therapeutic effect [24]. Furthermore, liver DCs showed higher T cell proliferation ability

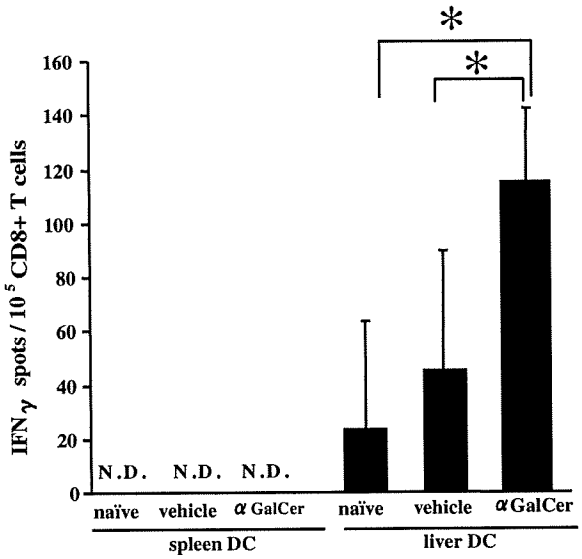

Fig. 5. Evaluation of $p53_{232-240}$ peptide specific CD8+ CTL induction after vaccination of p53 peptide-pulsed DCs from each treated mice. Normal BALB/c mice were immunized i.p. with 1×10^6 $p53_{232-240}$ peptide pulsed liver or spleen DCs isolated from α-GalCer or vehicle treated mice. Five days after vaccination, CD8+ T cells were isolated from the spleen of immunized mice. The frequency of $p53_{232-240}$ peptide specific CD8+ CTL was evaluated by IFN-γ ELSIPOT assay. The results are shown as spots/100,0000 CD8+ T cells; mean ± SD of triplicate samples. CD8+ T cell reactivity against peptide-unpulsed BMDCs served as the negative control in all cases, and this value was subtracted from all experimental determination to determine p53-specific spot numbers. $^*p < 0.05$. N.D., not detected. Similar results were obtained from three separate experiments.

than spleen DCs after α-GalCer treatment. Taken together, these results suggested that α-GalCer treatment resulted in the efficient activation of liver DCs more strongly than spleen DC, which might be associated with the induction of antitumor acquired immunity in the liver.

To examine whether the α-GalCer activated liver and spleen DCs could actually induce acquired immunity, we vaccinated $p53_{232-240}$ peptide-pulsed α-GalCer activated liver and spleen DCs. The frequencies of CD8+ T cells in response to $p53_{232-240}$ peptide were much higher in α-GalCer activated liver DCs vaccinated mice than those in vehicle-treated liver DCs vaccinated mice. Interestingly, the vaccination of $p53_{232-240}$ peptide-pulsed spleen DCs isolated from both α-GalCer and vehicle-treated mice did not generate $p53_{232-240}$ peptide-specific CTL responses. These data suggested that the immunological microenvironment in the spleen may support DCs to be potentially very tolerogenic resulting in inability of generating acquired immunity. In marked contrast, liver DCs potentially have the ability of generating antitumor acquired immunity and that α-GalCer could markedly enhance this ability. A normal mouse liver contains lymphocytes that are usually enriched with 10% NKT cells in contrast to mouse spleen that contains only 2% NKT cells [25]. α-GalCer presented by DCs activates NKT cells upregulating CD40 ligand on NKT cells, which in turn leads to the activation of DCs [17]. Actually we confirmed that i.p. injection of α-GalCer activated equally well in both liver and spleen NKT cells (Sasakawa, unpublished data). Thus, the higher population of NKT cells in the liver may be associated with efficient activation of liver DCs after α-GalCer treatment, which might characterize the unique immunological responses in the liver.

Despite recent progress and early success with various types of immunotherapy, there is still significant room for improvement in these regimens against liver cancer. We demonstrated that liver is an immunologically unique organ that is favorable for generation of acquired antitumor immunity. We propose that α-GalCer treatment may be an attractive strategy for suppressing tumor growth in the liver and promoting regression of metastatic lesions in other organs.

Acknowledgements

This work was supported by a Grant-in-Aid from the Ministry of Education, Culture, Sports, Science and Technology of Japan, a Grant-in-Aid for Research on Hepatitis and BSE from the Ministry of Health, Labor and Welfare of Japan and Core Research for Evolutional Science and Technology (CREST) from Japan Science and Technology Agency. The authors thank Kirin Pharma (Gunma, Japan) for providing the α-galactosylceramide.

Supplementary data

Supplementary data associated with this article can be found, in the online version, at doi:10.1016/j.jhep.2008.12.027.

References

[1] Kawano T, Cui J, Koezuka Y, Toura I, Kaneko Y, Sato H, et al. CD1d-restricted and TCR-mediated activation of Vα14NKT cells by glycosylceramides. Science 1997;278:1626–1629.
[2] Fujii S, Shimizu K, Kronenberg M, Steinman RM. Prolonged IFN-γ-producing NKT response induced with alpha-galactosylceramide-loaded DCs. Nat Immunol 2002;3:867–874.
[3] Miyagi T, Takehara T, Tatsumi T, Kanto T, Suzuki T, Jinushi M, et al. CD1d-mediated stimulation of natural killer T cells selectively activates hepatic natural killer cells to eliminate experimentally disseminated hepatoma cells in murine liver. Int J Cancer 2003;106:81–89.
[4] Nakagawa R, Motoki K, Ueno H, Iijima R, Nakamura H, Kobayashi E, et al. Treatment of hepatic metastasis of the colon26 adenocacinoma with an α-galactosylceramide, KRN7000. Cancer Res 1998;58:1202–1207.
[5] Nieda M, Okai M, Tazbirkova A, Lin H, Yamaura A, Ide K, et al. Therapeutic activation of Vα24+Vβ11+NKT cells in human

subjects results in highly coordinates secondary activation of acquired and innate immunity. Blood 2004;103:383–389.
[6] Giaccone G, Punt CJ, Ando Y, Ruijter R, Nishi N, Peters M, et al. A phase I study of the natural killer T-cell ligand α-galactosylceramide (KRN7000) in patients with solid tumors. Clin Cancer Res 2002;8:3702–3709.
[7] Steinman RM. The dendritic cell system and its role in immunogenicity. Annu Rev Immunol 1991;9:271–296.
[8] Hart DN. Dendritic cells: unique leukocyte populations which control the primary immune response. Blood 1997;90:3245–3287.
[9] Fujii S, Shimizu K, Smith C, Bonifaz L, Steinman RM. Activation of natural killer T cells by alpha-galactosylceramide rapidly induces the full maturation of dendritic cells in vivo and thereby acts as an adjuvant for combined CD4 and CD8 T cell immunity to a coadministered protein. J Exp Med 2003;198:267–279.
[10] Fujii S, Liu K, Smith C, Bonito AJ, Steinman RM. The linkage of innate to adaptive immunity via maturing dendritic cells in vivo requires CD40 ligation in addition to antigen presentation and CD80/86 costimulation. J Exp Med 2004;199:1607–1618.
[11] Shortman K, Liu TJ. Mouse and human dendritic cell subtypes. Nat Rev Immunol 2002;2:151–161.
[12] Nakagawa R, Nagafune I, Tazunoki Y, Ehara H, Tomura H, Iijima R, et al. Mechanisms of the antimetastatic effect in the liver and of the hepatocyte injury induced by alpha-galactosylceramide in mice. J Immunol 2001;166:6578–6584.
[13] Nakagawa R, Inui T, Nagafune I, Tazunoki Y, Motoki K, Yamauchi A, et al. Essential role of bystander cytotoxic CD122+CD8+ T cells for the antitumor immunity induced in the liver of mice by alpha-galactosylceramide. J Immunol 2004;172:6550–6557.
[14] Mayordomo JI, Loftus DJ, Sakamoto H, De Cesare CM, Appasamy PM, Lotze MT, et al. Therapy of murine tumors with p53 wild-type and mutant sequence peptide-based vaccines. J Exp Med 1996;183:1357–1365.
[15] Tatsumi T, Takehara T, Yamaguchi S, Sasakawa A, Sakamori R, Ohkawa K, et al. Intrahepatic delivery of α-galatosylceramide pulsed dendritic cells suppresses liver tumor. Hepatology 2007;45:22–30.
[16] Yamaguchi S, Tatsumi T, Takehara T, Sakamori R, Uemura A, Mizushima T, et al. Immunotherapy of murine colon cancer using receptor tyrosine kinase EphA2-derived peptide-pulsed dendritic cell vaccines. Cancer 2007;110:1469–1477.
[17] Chaudhry UI, Katz SC, Kingham TP, Pillarisetty VG, Raab JR, Shah AB, et al. In vivo overexpression of Flt3 ligand expands and activates murine spleen natural killer dendritic cells. FASEB J 2006;20:982–984.
[18] Seino K, Motohashi S, Fujisawa T, Nakayama T, Taniguchi M. Natural killer T cell-mediated anti-tumor immune responses and their clinical application. Cancer Sci 2006;97:807–812.
[19] Vremec D, Shortman K. Dendritic cell subtypes in mouse lymphoid organs: cross-correlation of surface markers, changes with incubation, and differences among thymus, spleen, and lymph nodes. J Immunol 1997;159:565–573.
[20] Nastala CL, Edington HD, McKinney TG, Tahara H, Nalesnik MA, Brunda MJ, et al. Recombinant IL-12 administration induces tumor regression in association with IFN-gamma production. J Immunol 1994;153:1697–1706.
[21] Lasek W, Feleszko W, Golab J, Stoklosa T, Marczak TM, Dabrowska A, et al. Antitumor effects of the combination immunotherapy with interleukin-12 and tumor necrosis factor alpha in mice. Cancer Immunol Immunother 1997;45:100–108.
[22] Pillarisetty VG, Shah AB, Miller G, Bleier JI, DeMatteo RP. Liver dendritic cells are less immunogenic than spleen dendritic cells because of differences in subtype composition. J Immunol 2004;172:1009–1017.
[23] Markus G, Traver D, Miyamoto T, Weissman IL, Akashi K. Dendritic cell potentials of early lymphoid and myeloid progenitors. Blood 2001;97:3333–3341.
[24] Belardelli F, Ferrantini M. Cytokines as a link between innate and adaptive antitumor immunity. Trends Immunol 2002;23:201–208.
[25] Doherty DG, O'Farrelly C. Innate and adaptive lymphoid cells in human liver. Immunol Rev 2000;174:5–20.

Anticancer Chemotherapy Inhibits MHC Class I–Related Chain A Ectodomain Shedding by Downregulating ADAM10 Expression in Hepatocellular Carcinoma

Keisuke Kohga, Tetsuo Takehara, Tomohide Tatsumi, Takuya Miyagi, Hisashi Ishida, Kazuyoshi Ohkawa, Tatsuya Kanto, Naoki Hiramatsu, and Norio Hayashi

Department of Gastroenterology and Hepatology, Osaka University Graduate School of Medicine, Osaka, Japan

Abstract

MHC class I–related chain A (MICA) is a ligand for the NKG2D-activating immunoreceptor that mediates activation of natural killer (NK) cells. The ectodomain of MICA is shed from tumor cells, which may be an important means of evading antitumor immunity. We previously reported that patients with hepatocellular carcinoma (HCC) display high levels of soluble MICA in circulation, which could be downregulated by chemotherapy. The present study shows that anti-HCC drugs suppress MICA ectodomain shedding by inhibiting expression of a disintegrin and metalloproteinase 10 (ADAM10). Both ADAM10 and CD44, a typical substrate of the ADAM10 protease, were expressed in human HCC tissues and HCC cells but not in normal liver tissues or cultured hepatocytes. Small interfering RNA–mediated knockdown experiments revealed that ADAM10 is a critical sheddase for both MICA and CD44 in HCC cells. Of interest is the finding that epirubicin clearly downregulated ADAM10 expression and MICA shedding in HCC cells; its suppressive effect on MICA shedding was abolished in ADAM10-depleted cells. Epirubicin treatment also enhanced the NKG2D-mediated NK sensitivity of HCC cells. Patients with HCC had significantly higher levels of serum-soluble CD44, which correlated well with serum-soluble MICA levels, thus suggesting a close link between ADAM10 activity and MICA shedding in these patients. Soluble MICA and CD44 levels were downregulated with a significant correlation in patients treated by transarterial chemoembolization using epirubicin. In conclusion, anticancer drugs can modulate expression of ADAM10, which is critically involved in MICA ectodomain shedding. Epirubicin therapy may have a previously unrecognized effect on antitumor immunity in HCC patients. [Cancer Res 2009;69(20):8050–7]

Introduction

Hepatocellular carcinoma (HCC) is one of the leading causes of cancer deaths worldwide. Chronic liver disease caused by hepatitis virus infection and nonalcoholic steatohepatitis leads to a predisposition for HCC, with liver cirrhosis, in particular, being considered a premalignant condition (1, 2). With regard to treatment, surgical resection or percutaneous techniques such as ethanol injection and radiofrequency ablation are considered to be choices for curable treatment of localized HCC, whereas transcatheter arterial chemoembolization (TACE) is a well-established technique for more advanced HCC (3). The liver contains a large compartment of innate immune cells [natural killer (NK) cells and natural killer T cells] and acquired immune cells (T cells; refs. 4, 5), but the activation of these immune cells after HCC treatments remains unclear. If such treatments can efficiently activate abundant immune cells in the liver, this could lead to the establishment of attractive new strategies for HCC treatment.

MHC class I–related chain A and B (MICA and MICB) are ligands for NKG2D expressed on a variety of immune cells (6). In contrast to classic MHC class I molecules, MICA/B are rarely expressed on normal cells but frequently on tumor cells (7–10). The engagement of MICA/B and NKG2D strongly activates NK cells and costimulates T cells, enhancing their cytolytic activity and cytokine production (11). Thus, the MICA/B-NKG2D pathway is an important mechanism by which the host immune system recognizes and kills transformed cells (12). In addition to those membrane-bound forms, MICA/B molecules are also cleaved proteolytically from tumor cells and appear as soluble forms in sera of patients with malignancy (13–15). Soluble MICA/B in circulation downregulates NKG2D expression and disturbs NKG2D-mediated antitumor immunity (9, 10, 13). We previously reported that soluble MICA could be detected in sera of HCC patients (16) and that TACE treatment reduces the levels of soluble MICA and thereby upregulates the expression of NKG2D (17). Thus, cancer therapy may have a beneficial effect on NKG2D-mediated immune responses.

The release of soluble MICA/B from tumor cells is impaired by metalloproteinase inhibitors, suggesting the involvement of members of the metzincin superfamily, such as ADAM proteins (14, 18). In addition, ERp5, related to protein disulfide isomerase, is required for the MICA shedding as it reduces disulfide bond of the α3 domain of MICA (19). Although it may not be a direct protease for MICA, it may enable proteolytic cleavage through conformational change. Recently, it was reported that MICA shedding of 293T fibroblast cells and HeLa cervical cancer cells was inhibited by silencing of the ADAM10 and ADAM17 proteases (20). This suggests that ADAM family proteins may be a therapeutic target for enhancing antitumor immunity, but how to therapeutically modulate these proteins is still not clear. Furthermore, it remains to be determined whether ADAMs can regulate MICA shedding in a clinical setting.

In the present study, we showed that ADAM10, but not ADAM17, was critically required for MICA shedding in human HCC cells. Of importance is the discovery that epirubicin, a widely used anti-HCC drug, was capable of downregulating ADAM10 expression and

Note: Supplementary data for this article are available at Cancer Research Online (http://cancerres.aacrjournals.org/).

K. Kohga, T. Takehara, and T. Tatsumi contributed equally to this work.

Requests for reprints: Norio Hayashi, Department of Gastroenterology and Hepatology, Osaka University Graduate School of Medicine, 2-2 Yamadaoka, Suita, Osaka 565-0871, Japan. Phone: 81-6-6879-3621; Fax: 81-6-6879-3629; E-mail: hayashin@gh.med.osaka-u.ac.jp.

doi:10.1158/0008-5472.CAN-09-0789

activity in HCC cells; it can thus inhibit MICA shedding and enhance NK sensitivity. ADAM10 was immunohistochemically detected in HCC tissues and a correlation was observed between soluble MICA levels and ADAM10 activity determined by soluble CD44 levels in HCC patients. The present study sheds light on previously unrecognized effects of an anticancer drug on modulating ADAM family proteins and MICA shedding and thus suggests a promising aspect for chemoimmunotherapy against human HCC.

Materials and Methods

Liver tissues and immunohistochemistry. Human HCC tissues (n = 8) and normal liver tissues (n = 2) obtained at surgical resection were used. Informed consent, under an institutional review board–approved protocol,

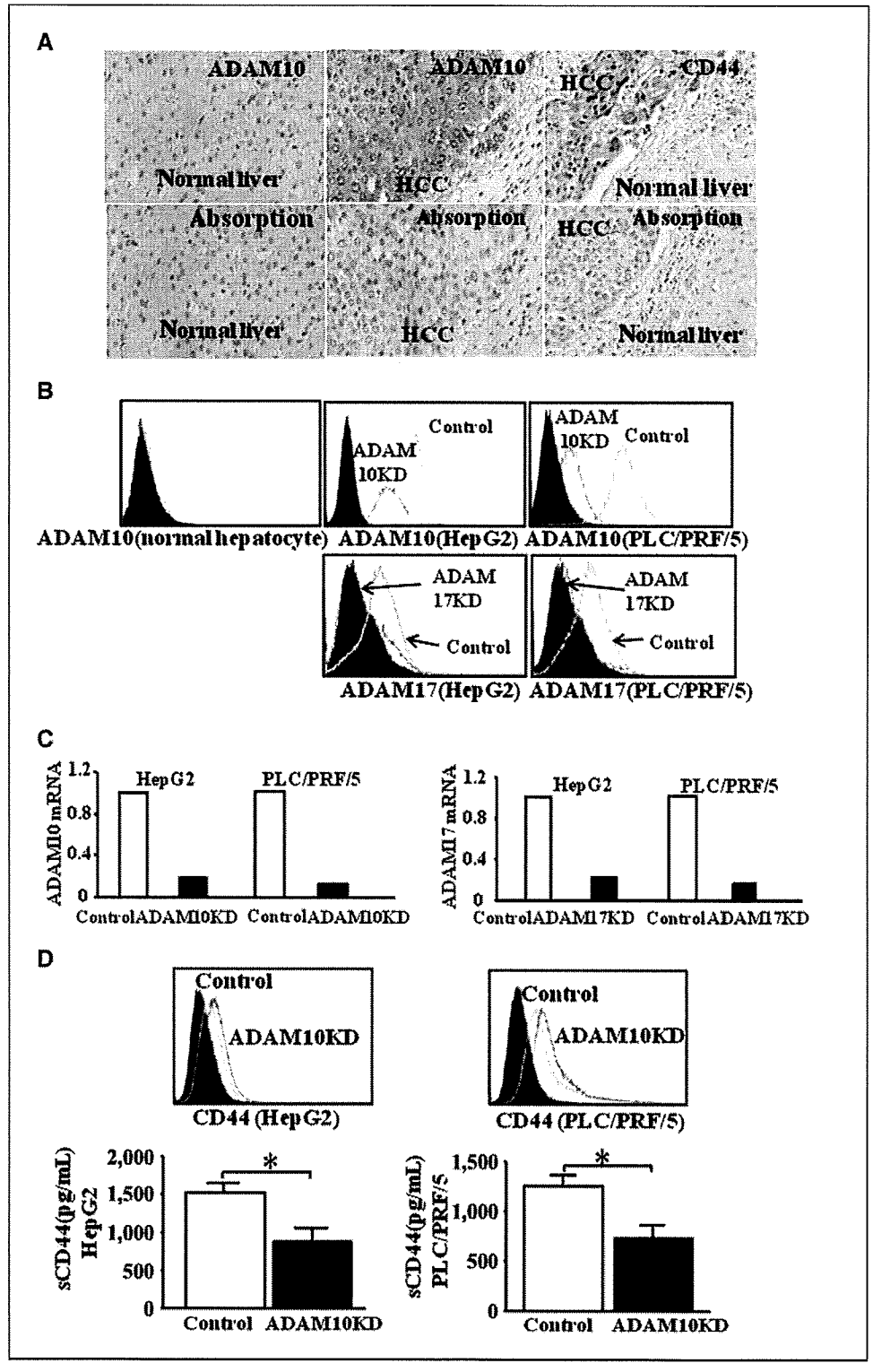

Figure 1. Expression of ADAM10 and CD44 in human HCC tissues and ADAM10 or ADAM17 knockdown in human HCC cells. *A*, immunohistochemical detection of ADAM10 and CD44 in human HCC tissues (n = 8) and normal liver tissues (n = 2). Liver sections were stained with the corresponding antibodies (*top panels*). Both primary antibodies were incubated with recombinant CD44 and ADAM10 proteins and then applied to liver sections in parallel as the absorption test (*bottom panels*). Representative images are shown. *B* and *C*, expression of ADAM10 or ADAM17 in human primary hepatocyte and HCC cell lines (*HepG2* and *PLC/PRF/5*). Cells were treated with ADAM10 siRNA, ADAM17 siRNA, or control siRNA, and subjected to analysis of ADAM10 or ADAM17 expression by flow cytometry (*B*) or real-time RT-PCR (*C*). *Histograms,* anti-ADAM10 or anti-ADAM17 staining of ADAM10 or ADAM17 siRNA-treated cells (*ADAM10KD* or *ADAM17KD, black dotted line*) and control siRNA-treated cells (*Control, gray line*), respectively. *Closed histograms,* control IgG staining. *D,* the expression of membrane-bound CD44 on HCC cells treated with ADAM10 siRNA (ADAM10KD, *black line*) or control siRNA (*Control, gray line*) was evaluated by flow cytometry (*top panels*). *Closed histograms,* control IgG staining. Soluble CD44 (*sCD44*) production from HCC cells treated with ADAM10 siRNA or control siRNA were evaluated by specific ELISA (*bottom panels*). *, $P < 0.05$.

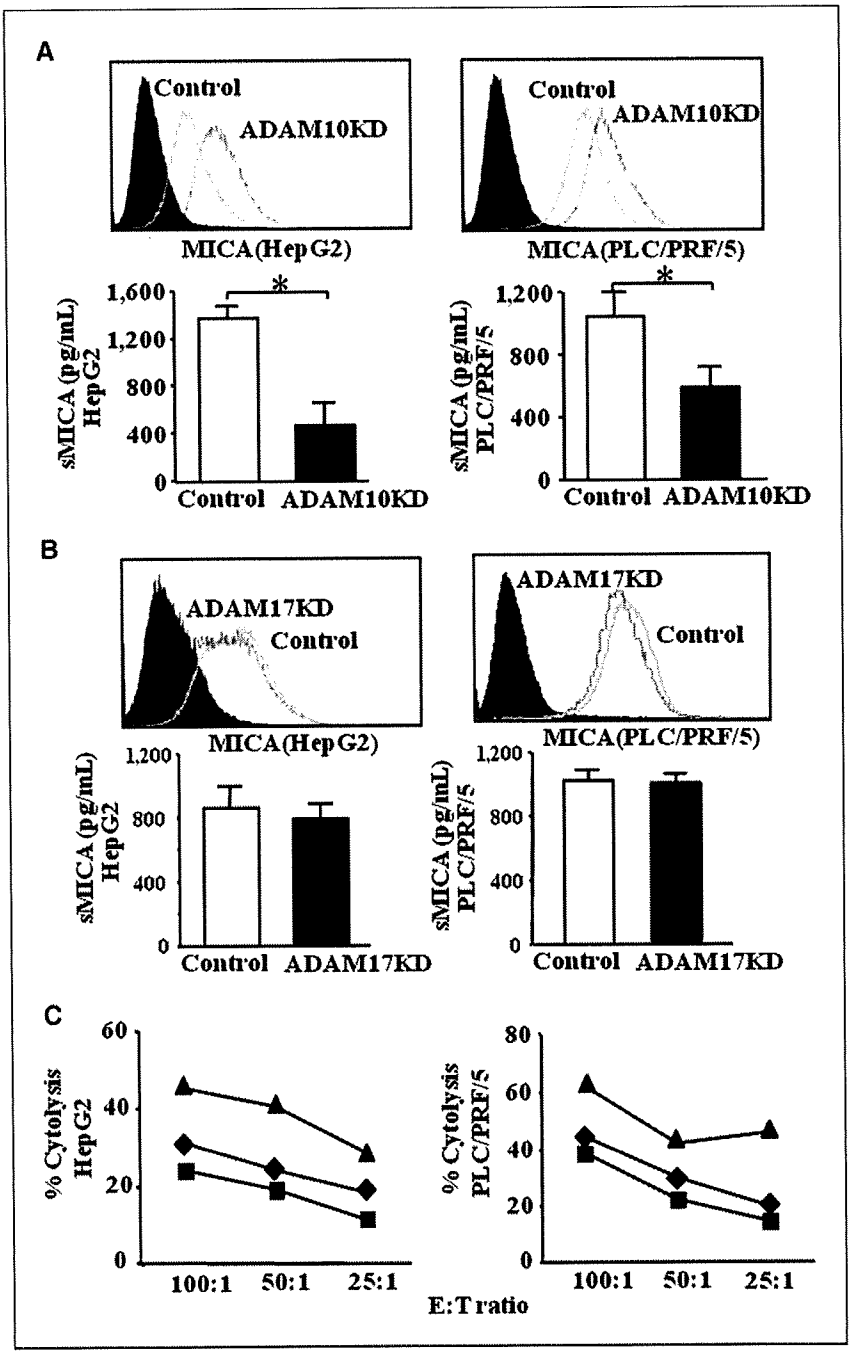

Figure 2. Expression of MICA in ADAM10 or ADAM17 knockdown HCC cells and NK sensitivity in ADAM10 knockdown HCC cells. *A* and *B*, the expression of membrane-bound MICA on HCC cells treated with ADAM10 siRNA (*ADAM10KD, black line*; *A*), ADAM17 siRNA (*ADAM17KD, black line*; *B*), or control siRNA (*Control, gray line*) was evaluated by flow cytometry (*top panels*). *Closed histograms*, control IgG staining. Soluble MICA (*sMICA*) production from HCC cells treated with ADAM10 siRNA (*A*), ADAM17 siRNA (*B*), or control siRNA were evaluated by specific ELISA (*bottom panels*). *, $P < 0.05$. *C*, HCC cells treated with ADAM10 siRNA or control siRNA were subjected to ^{51}Cr-release assay against NK cells. Cytolytic activity of NK cells against control HCC cells (■) or ADAM10 knockdown HCC cells without (▲) or with blocking antibody of MICA/B (6D4; ♦). Representative results are shown. Similar results were obtained from three independent experiments.

was obtained from all patients before sample acquisition. Liver sections were subjected to immunohistochemical staining using the ABC procedure (Vector Laboratories, Burlingame, CA). The primary antibodies used were anti-ADAM10 and anti-CD44 (R&D Systems). To confirm the specificity of the staining, primary antibodies were incubated with recombinant CD44 or ADAM10 protein (R&D Systems, Minneapolis, MN) for 3 h and then applied onto liver sections in parallel with staining of the primary antibodies as the absorption test.

HCC cell lines. Human HCC cell lines HepG2 and PLC/PRF/5 were purchased from the American Type Culture Collection and were cultured with DMEM supplemented with 10% fetal bovine serum (GIBCO/Life Technologies, Grand Island, NY) in a humidified incubator at 5% CO_2 and 37°C.

RNA silencing. The small interfering RNA (siRNA) method was used to knockdown ADAM10 and ADAM17. Stealth RNAi oligonucleotide targeting ADAM10 or ADAM17 and scrambled oligonucleotides as a control were purchased from Invitrogen (Carlsbad, CA). Cells were transfected by RNAi Max transfection reagent (Invitrogen) with 50 nmol/L siRNA. At 24 h posttransfection, the cells were analyzed for specific depletion of the mRNAs of ADAM10 and ADAM17 by real-time reverse transcription-PCR (RT-PCR; Applied Biosystems, Foster City, CA). The following siRNAs were used: ADAM10, 5′-AUAUCUGGGCAAUCACAG-CUUCUCG-3′; scramble control, 5′-AUACUUGGUCAACGCACUUCGAUGG-3′; ADAM17, 5′-UGAACAAGCUCUUCAGGUGGUUCUC-3′; scramble control, 5′-UGAUUAGAACUCUCGACUGGUGCUC-3′.

ELISA. The supernatants of cultured cells were harvested at 24 h after transfection with siRNA as well as sera from HCC patients (n = 97) and age-matched healthy volunteers (n = 32) were subjected to analysis of soluble MICA and soluble CD44 levels. Informed consent, under an institutional review board–approved protocol, was obtained from all patients before sample acquisition. The levels of soluble MICA and soluble CD44 were

determined by DuoSet MICA eELISA kit (R&D Systems) and soluble CD44std ELISA (Abcam, Cambridge, MA), respectively.

Flow cytometry. For the detection of membrane-bound MICA and CD44, cells were incubated with an anti-MICA–specific antibody (2C10, Santa Cruz Biotechnology, Santa Cruz, CA) or anti-CD44 antibody (R&D Systems) and stained with phycoerythrin (PE)-goat anti-mouse immunoglobulin (Beckman Coulter) as a secondary reagent and then subjected to flow cytometric analysis. For the detection of ADAM10 or ADAM17, cells were fixed and permeabilized with Cytofix/Cytoperm (BD Biosciences, San Jose, CA) and stained with PE-conjugated anti-ADAM10 or anti-ADAM17 antibody (R&D Systems). Flow cytometric analysis was performed using a FACScan flow cytometer (Becton Dickinson).

Plasmid construction of pMyc-MICA. MICA full coding cDNA was isolated from Huh7, human HCC cells, using a conventional RT-PCR method (Supplementary Fig. S1, DDBJ/EMBL/Genbank accession number AB506764) and inserted into the *Hin*dIII-*Xba*I site of pcDNA3 (Invitrogen). A C-myc tag was placed between the leader peptide and the α1 domain of MICA by site-specific mutagenesis using a QuikChange site-directed mutagenesis kit (Stratagene, La Jolla, CA) referred to as pMyc-MICA. Cells were transfected with pMyc-MICA using a Lipofectamine LTX reagent (Invitrogen). The green fluorescent protein (GFP)–expressing vector (pEGFP-C1, Clontech, Mountain View, CA) was cotransfected to evaluate the transfection efficiency.

Immunoprecipitation. Cells or tissues were homogenized in lysis buffer containing 1% NP40, 0.5% sodium deoxycholate, 0.1% SDS, 50 μg/mL aprotinin, 100 μg/mL phenylmethylsulfonyl fluoride, 1 mmol/L sodium orthovanadate, 50 mmol/L sodium fluoride, and PBS. To the cell supernatants, 0.5% NP40 and a cocktail of protease inhibitors were added. The protein contents of the samples were determined by BCA protein assay kit (Pierce, Rackford, IL). Immunoprecipitation with anti–c-Myc beads was performed for 1 h at 4°C. Immunocomplexes were eluted by a c-Myc–tagged peptide solution (MBL, Woburn, MA). The samples after immunoprecipitation were treated with 250 mU of N-glycosidase F (Roche, Mannheim, Germany) for 3 h at 37°C.

Western blotting. The total cellular protein was electrophoretically separated using SDS-12% polyacrylamide gels and transferred onto polyvinylidene difluoride membrane. The membrane was blocked in TBS-Tween containing 5% skim milk for 1 h and then probed with anti-Myc mouse monoclonal antibody (Cell Signaling Technology, Danvers, MA) at 4°C overnight. Horseradish peroxidase–conjugated anti-rabbit antibody and SuperSignal West Pico System (Pierce) were used for the detection of blots.

Real-time RT-PCR. Total RNA was isolated using RNeasy Mini Kit (Qiagen K.K., Tokyo, Japan) and was reverse transcribed using SuperScript III First-Strand Synthesis System (Invitrogen). The mRNA levels were evaluated using ABI PRISM 7900 Sequence Detection System (Applied Biosystems). Ready-to-use assays (Applied Biosystems) were used for the quantification of ADAM10 (Hs00153853_m1), ADAM17 (Hs00234221_m1), MICA (Hs00792195_m1), β-actin (Hs99999903_m1), and CD44 (Hs00174139_m1) mRNAs according to the manufacturer's instructions. The thermal cycling conditions for all genes were 2 min at 50°C and 10 min at 95°C, followed by 40 cycles at 95°C for 15 s and 60°C for 1 min. β-Actin mRNA from each sample was quantified as an endogenous control of internal RNA.

WST-8 assay. HepG2 and PLC/PRF/5 cells were treated with different concentrations of epirubicin for 24 h. Cell growth of epirubicin-treated HCC cells was determined by WST-8 assay (Nacalai Tesque, Kyoto, Japan) as previously described (21).

NK cell analysis. NK cells were isolated from human peripheral blood mononuclear cells by magnetic cell sorting using CD56 MicroBeads (Miltenyl Biotech, Auburn, CA) as previously described (16). The cytolytic ability of NK cells was assessed by 4-h ^{51}Cr-releasing assay with or without MICA/B-blocking antibody (6D4; ref. 7), which binds to the α1 and α2 domains of MICA and MICB. 6D4 was a generous gift from Drs. Veronika Groh and Thomas Spies (Fred Hutchinson Cancer Research Center, Seattle, WA).

Statistics. All values were expressed as the mean and SD. The statistical significance of differences between the groups was determined by applying Student's *t* test or two-sample *t* test with Welch correction after each group

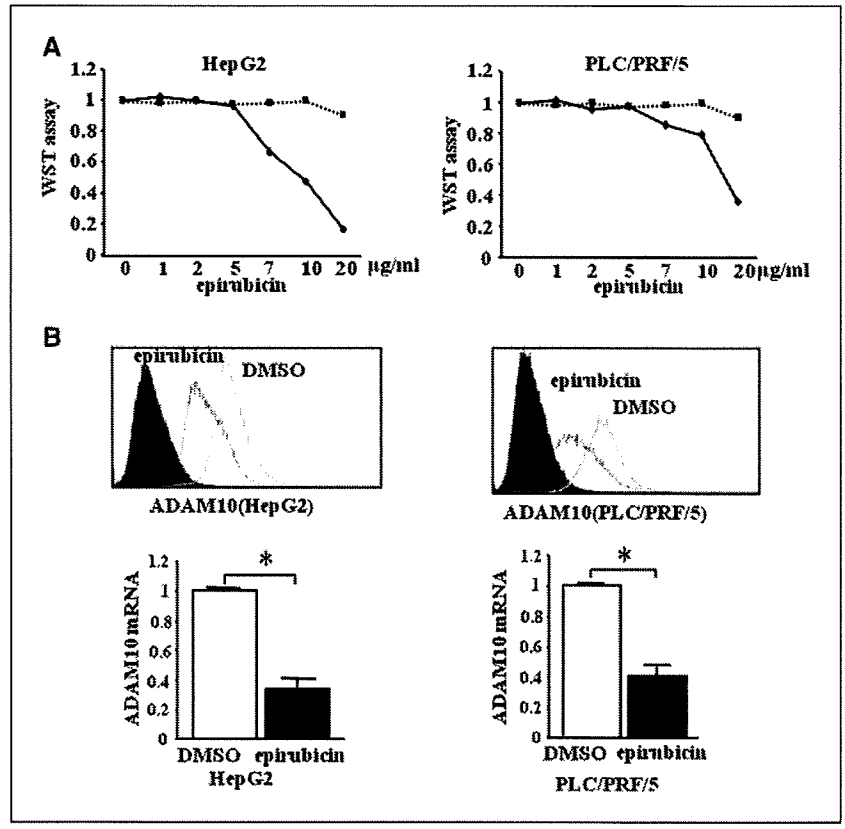

Figure 3. Expression of ADAM10 in epirubicin-treated HCC cells. *A*, the cytotoxicity of epirubicin to human HCC cells was evaluated by WST-8 assay. Cells were treated with different doses of epirubicin (*solid lines*) or vehicle (*DMSO*; *dotted lines*) for 24 h, and the viability of the cells was evaluated by the WST-8 assay. *B*, ADAM10 expression of epirubicin-treated HCC cells. Cells were treated with a nontoxic dose of 1 μg/mL epirubicin (*black lines*) or vehicle (DMSO, *gray lines*) for 24 h and their ADAM10 expression was evaluated by flow cytometry (*top panels*). *Closed histograms*, control IgG staining. Total RNA was extracted at 24 h of epirubicin treatment and mRNA levels of ADAM10 were evaluated by real-time RT-PCR (*bottom panels*). *, $P < 0.05$.

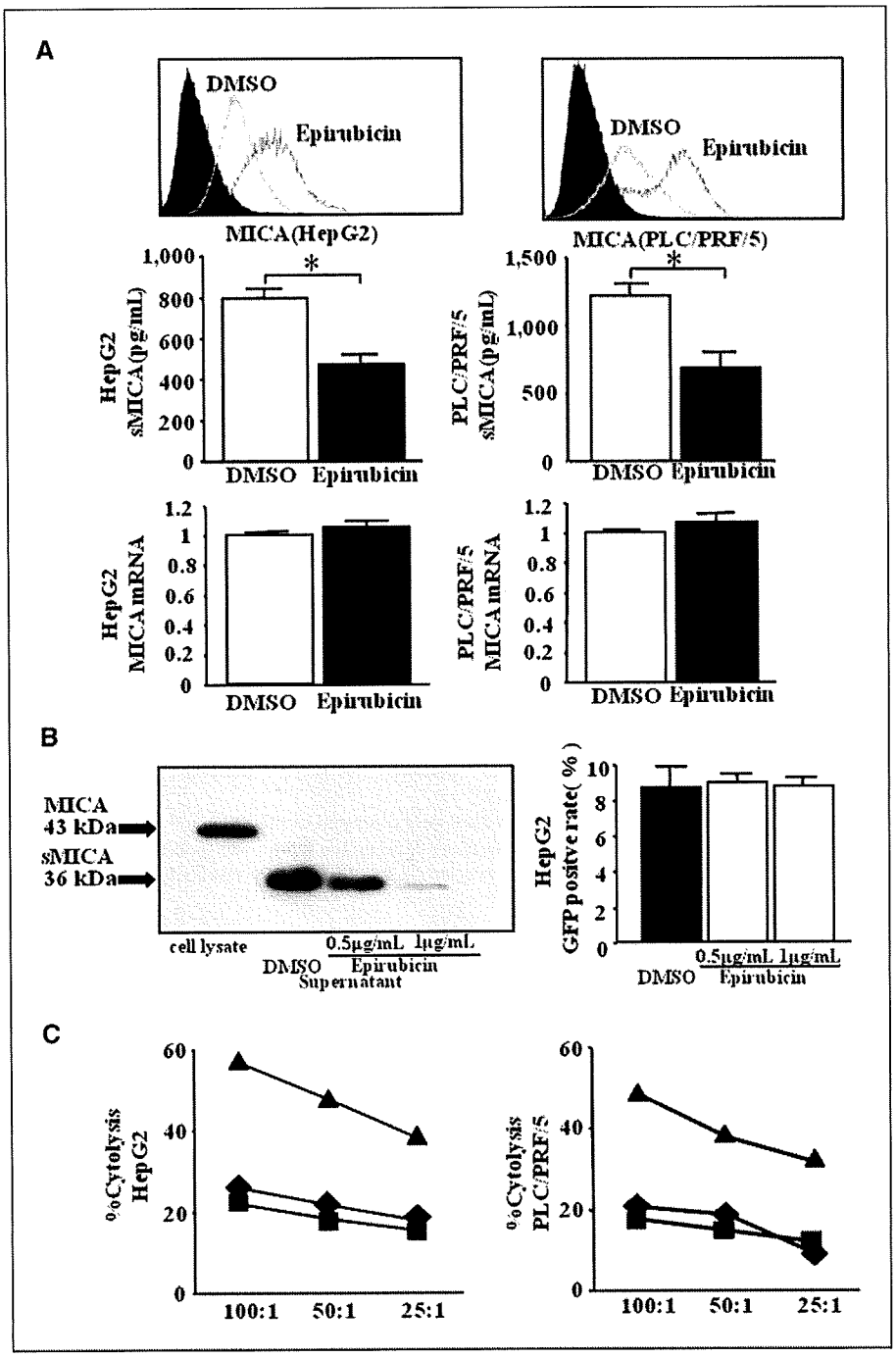

Figure 4. Expression and shedding of MICA in epirubicin-treated HCC cells. *A*, HCC cells were treated with a nontoxic dose of 1 μg/mL epirubicin (*black lines*) or vehicle (DMSO, *gray lines*) for 24 h and their expression of membrane-bound MICA and MICA mRNA was evaluated by flow cytometry (*top panels*) and real-time RT-PCR (*bottom panels*), respectively. *Closed histograms*, control IgG staining in flow cytometry. At the same time, 24-h culture supernatants were subjected to the analysis of soluble MICA (*sMICA*) levels by ELISA (*middle panels*). *, $P < 0.05$. *B*, HepG2 cells were transfected with pMyc-MICA and pEGFP-C1, cultured with 0.5 to 1 μg/mL epirubicin or vehicle (DMSO) for 24 h. Cell lysates from HepG2 cells and 24-h culture supernatants of epirubicin- or vehicle-treated HepG2 cells were immunoprecipitated with anti-Myc. The resulting immunoprecipitates were eluted, treated with N-glycanase, and subjected to Western blot analysis for MICA (*left*). Transfection efficacies were equal in all treatment groups as evidenced by similar GFP-positive cell rates (*right*). *C*, the cytolytic activity of NK cells against HCC cells. Vehicle-treated cells (■) or epirubicin-treated cells without (▲) or with blocking antibody of MICA/B (6D4; ♦) were subjected to ^{51}Cr-release assay. Representative results are shown. Similar results were obtained from three independent experiments.

had been tested with equal variance and Fisher's exact probability test. We defined statistical significance as $P < 0.05$.

Results

ADAM10 and CD44 are overexpressed in human HCC. ADAM10 was detected in all human HCC tissues tested by immunohistochemistry but not in normal liver tissues (Fig. 1*A*). Flow cytometric analysis revealed that ADAM10 was strongly expressed in a variety of HCC cell lines, including HepG2, PLC/PRF/5 (depicted in Fig. 1*B*), and Hep3B (data not shown), but faintly in primary hepatocytes. CD44, a typical substrate of the ADAM10 protease, was also expressed in all human HCC tissues but not in normal liver tissues (Fig. 1*A*). The data suggest that overexpression of ADAM10 and CD44 is a characteristic of human HCC like other malignancies (22).

ADAM10 is involved in MICA shedding of HCC cells but ADAM17 is not. To examine the involvement of ADAM family proteins in MICA ectodomain shedding, ADAM10 or ADAM17 were knocked down in HCC cells using a siRNA-mediated procedure. ADAM10 expression was clearly suppressed in HepG2 cells and PLC/PRF/5 cells at both mRNA and protein levels (Fig. 1*B* and *C*). Both cell lines expressed CD44 on the cellular surface and produced significant levels of soluble CD44 (Fig. 1*D*), indicating that CD44 is expressed and shed from those cell lines. ADAM10 knockdown (KD)

led to an increase in CD44 expression on HCC cells and a decrease in soluble CD44 levels in culture supernatants (Fig. 1*D*). Because ADAM10 has been established as being a sheddase for CD44, siRNA-mediated knockdown of ADAM10 suppressed not only the expression but also the activity of ADAM10 in HCC cells. HepG2 and PLC/PRF/5 cells also expressed ADAM17, which was clearly knocked down by a siRNA-mediated procedure (Fig. 1*B*).

HepG2 cells and PLC/PRF/5 cells expressed membrane-bound MICA and also produced soluble MICA (Fig. 2*A*). Knockdown of ADAM10 for both cell lines clearly upregulated MICA expression on their cellular surface and downregulated soluble MICA levels in their culture supernatant (Fig. 2*A*). In contrast, knockdown of ADAM17 did not affect the expression of membrane-bound MICA or the production of soluble MICA (Fig. 2*B*). We also examined the involvement of ADAM17 in MICA shedding of phorbol 12-myristate 13-acetate (PMA)–stimulated HCC cells because ADAM17 is considered to primarily affect stimulated shedding. The expression of membrane-bound MICA and the soluble MICA production were equal between PMA-stimulated ADAM17KD-HCC cells and control HCC cells (Supplementary Fig. S2). Thus, ADAM10, but not ADAM17, is critically involved in the shedding of MICA in HCC cells.

We next evaluated the cytolytic activity of NK cells against HCC cells. The cytolytic activity of NK cells against ADAM10KD-HepG2 cells was higher than that against control HepG2 cells. This activity was inhibited by blocking of anti-MICA/B antibody, suggesting that the increase of NK sensitivity depended on the increased expression of membrane-bound MICA on ADAM10KD-HepG2 cells, although we could not exclude the possibility of the involvement of MICB in this cytotoxicity (Fig. 2*C*). Similar results were also obtained with ADAM10KD-PLC/PRF/5 cells.

Epirubicin suppresses ADAM10 expression in HCC cells. We examined the biological modification of human HCC cells by adding epirubicin, which is commonly used in anti-HCC chemotherapy. We first examined the cytotoxicity of epirubicin to human HCC cells by WST-8 assay. Adding >5 μg/mL of epirubicin resulted in a significant decrease in cell growth of both HepG2 and PLC/PRF/5 cells (Fig. 3*B*). Based on these findings, we used 1 μg/mL of epirubicin to evaluate the biological effect on human HCC cells without toxicity. Both HepG2 cells and PLC/PRF/5 cells were cultured for 24 h with epirubicin and then subjected to analysis of ADAM10 expression. Epirubicin suppressed ADAM10 expression at the mRNA and protein levels in both cell lines (Fig. 3*C*). Although the data are not shown, doxorubicin also suppressed ADAM10 expression in HCC cells.

Epirubicin inhibits MICA ectodomain shedding and enhances susceptibility to NK cells of HCC cells. The above observations led us to investigate whether epirubicin or doxorubicin treatment would affect MICA ectodomain shedding in HCC cells. Epirubicin treatment led to an increase in membrane-bound MICA expression and a decrease in soluble MICA production in both HepG2 and PLC/PRF/5 cells (Fig. 4*A*). The mRNA levels of MICA did not change after exposure to epirubicin in both HCC cells (Fig. 4*A*). Similar data were obtained with doxorubicin-treated cells (data not shown).

To confirm whether the soluble MICA detected by ELISA was actually reflected in the cleaved form, we transfected Myc-tagged MICA into HepG2 cells and collected culture supernatants as well as cellular lysates. Immunprecipitates from these samples with anti-Myc were subjected to Western blot analysis after treatment with N-glycosidase. MICA in the culture supernatants migrated faster than cellular MICA (Fig. 4*B*), indicating that the MICA detected by ELISA is actually processed and released from full-length MICA. Epirubicin treatment led to a decrease in soluble MICA protein in HepG2 cells (Fig. 4*B*).

We next evaluated whether the epirubicin treatment could also modify the NK sensitivity of human HCC cells. Epirubicin-treated HepG2 cells or PLC/PRF/5 cells were more susceptible to NK cells than nontreated HepG2 or PLC/PRF/5 cells (Fig. 4*C*). The cytolytic activity against epirubicin-treated HCC cells was significantly decreased to the control levels by adding the anti-MICA/B blocking antibody. These results showed that the addition of epirubicin enhanced the NK sensitivity of HCC cell through increased

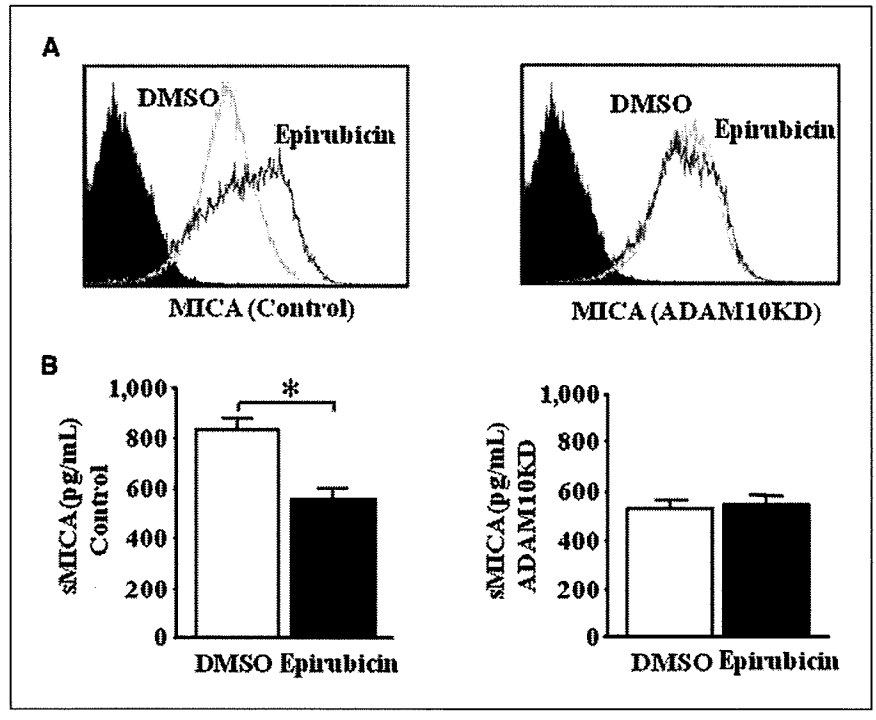

Figure 5. The epirubicin-mediated modification of MICA is ADAM10 dependent. HepG2 cells were transfected with ADAM10 siRNA (*ADAM10KD*) or control siRNA (*Control*) and further cultured with 1 μg/mL of epirubicin (*black lines*) or vehicle (DMSO, *gray line*) for 24 h. The expression of membrane-bound MICA (*MICA*) was evaluated by flow cytometry (*A*), and the soluble MICA (*sMICA*) production in the culture supernatant was evaluated by specific ELISA (*B*). Similar results were obtained from two independent experiments. *, $P < 0.05$.

expression of membrane-bound MICA, although the possibility of MICB involvement could not be excluded. The doxorubicin-treated human HCC cells showed similar results to those obtained from epirubicin-treated HCC cells (data not shown).

Epirubicin inhibits MICA ectodomain shedding through suppression of ADAM10. To examine whether the suppressive effect of epirubicin on MICA shedding occurred through downregulation of ADAM10, HepG2 cells were transfected with ADAM10 siRNA or scramble siRNA as a control and then treated with epirubicin. Consistent with earlier observations, epirubicin upregulated MICA surface expression and downregulated the levels of soluble MICA in control cells (Fig. 5). In contrast, neither upregulation of surface MICA nor downregulation of soluble MICA levels was observed in ADAM10KD-HepG2 cells. These results suggest that the suppressive effect of epirubicin on MICA shedding is mediated by ADAM10 downregulation. We also found similar results with ADAM10KD-PLC/PRF/5 cells (data not shown).

Soluble CD44 and soluble MICA levels in patients with HCC. We have shown that ADAM10 is expressed in human HCC tissues. However, it is not clear whether ADAM10 activity in HCC tissues is actually involved in MICA shedding in patients. Because ADAM10 was reported to be the constitutive functional sheddase of CD44 (23), we examined the soluble CD44 levels in HCC patients, which might be produced from tumor cells through ADAM10 activity. As shown in Fig. 6*A*, the soluble CD44 levels in HCC patients (n = 97) were significantly higher than those in age-matched healthy volunteers (n = 32). More importantly, soluble MICA levels in HCC patients significantly correlated with soluble CD44 levels (Fig. 6*B*), suggesting a close link between MICA shedding and ADAM10 activity.

We further examined soluble CD44 levels before and 2 weeks after TACE in HCC patients. Whereas the levels did not change in nontreated HCC patients during the 2-week interval (n = 9; 306.7 ± 82.5 ng/mL and 309.9 ± 79.9 ng/mL after 2 weeks), they were significantly decreased in epirubicin-based TACE-treated HCC patients (n = 21; 339.7 ± 78.1 ng/mL before TACE and 308.9 ± 81.4 ng/mL after TACE, $P < 0.003$). The changes of soluble CD44 in TACE treatment correlated significantly with those of soluble MICA (P = 0.0002; Fig. 6*C*). These results indicated that ADAM10-mediated CD44 shedding was decreased after TACE in HCC patients, implying that this reduction of ADAM10 activity might be related to the decline in MICA shedding.

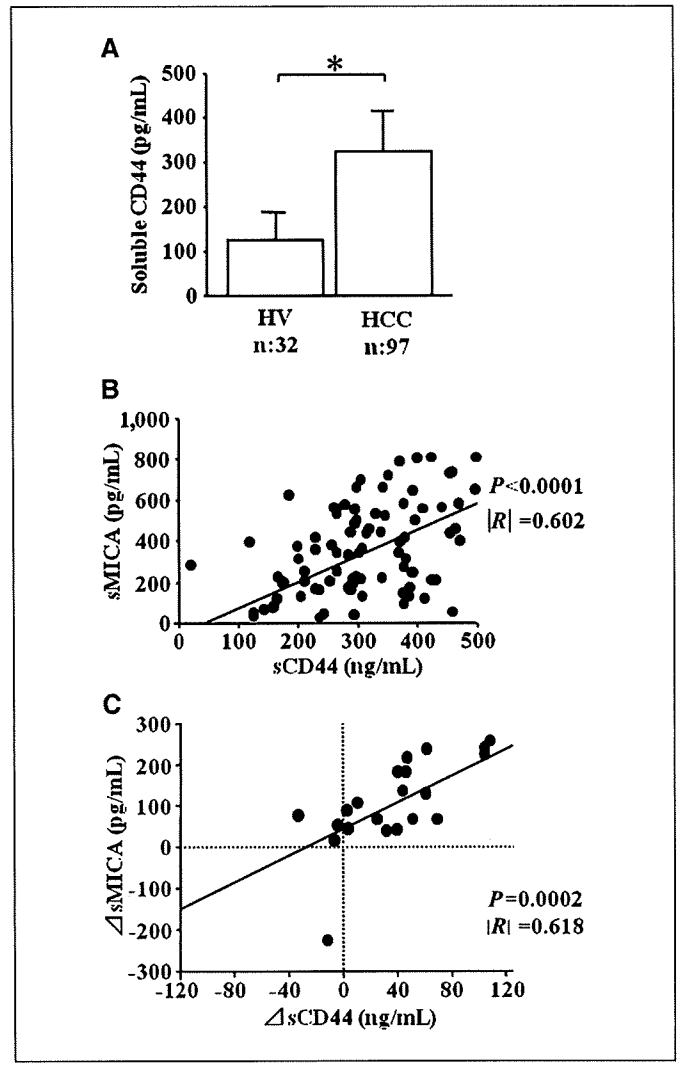

Figure 6. Correlation between soluble CD44 and soluble MICA in human HCC patients. *A* and *B*, soluble CD44 levels and MICA levels in healthy volunteers and HCC patients. Soluble CD44 levels (*sCD44*) and soluble MICA levels (*sMICA*) were determined for sera of HCC patients (n = 97) and age-matched healthy volunteers (*HV*; n = 32). *A*, comparison of sCD44 levels between groups; *B*, correlation between sCD44 levels and sMICA levels in 97 HCC patients. *, $P < 0.05$. *C*, correlation of sCD44 levels and sMICA levels during TACE therapy. HCC patients (n = 21) treated with epirubicin-based TACE therapy were enrolled and examined for sMICA and sCD44 levels before and 2 wk after therapy. Changes in sMICA (ΔsMICA = serum level of sMICA before TACE treatment − serum level of sMICA after TACE treatment) and those in sCD44 levels (ΔsCD44 = serum level of sCD44 before TACE treatment − serum level of sCD44 after TACE treatment) are plotted.

Discussion

MICA shedding is thought to be a principal mechanism by which tumor cells escape from NKG2D-mediated immunosurveillance (13). Thus, inhibition of MICA shedding should be a reasonable strategy for enhancing antitumor immunity. In the present study, we showed that ADAM10 was overexpressed in human HCC tissues and that ADAM10 knockdown resulted in increased expression of membrane-bound MICA, decreased production of soluble MICA, and upregulation of NK sensitivity of human HCC cells. These results point to ADAM10 as a therapeutic target for inhibiting MICA shedding, thereby ameliorating immunity against HCC. Waldhauer and colleagues recently showed that both ADAM10 and ADAM17 proteases are critically involved in the proteolytic release of soluble MICA of human 293T fibroblast cells and HeLa cervix carcinoma cells (20). Interestingly, in the present study, ADAM17 knockdown failed to affect MICA expression in human HepG2 cells or PLC/PRF/5 cells. Thus, ADAM10, not ADAM17, plays an essential role in the shedding of MICA in human HCC cells. Anderegg and colleagues (23) reported that only ADAM10, not ADAM17, contributed to shedding of CD44 molecules in human melanoma cells although both ADAM10 and ADAM17 proteases were significantly expressed in human melanoma tissues, suggesting that ADAM10 and ADAM17 do not always work in a similar manner. A recent report showed that ADAM10, but not ADAM17, could directly bind to calmodulin (24), which may involve the difference of MICA cleavage between ADAM10 and ADAM17 proteases. Recently, Boutet and colleagues reported that ADAM17 regulates proteolytic shedding of the MICB protein, which is another ligand for the NKG2D receptor on immune cells (25). We previously showed that both soluble MICA and MICB significantly increased in the sera of HCC patients and that therapeutic intervention for HCC leads to reduction of soluble

MICA levels, but not of soluble MICB levels (17), suggesting a more important role of soluble MICA in regulating NKG2D expression after HCC therapy. This led us to focus on the mechanism of MICA shedding in the present study.

Our results revealed that anticancer drugs such as epirubicin and doxorubicin downregulated ADAM10 expression and activity, thereby inhibiting MICA ectodomain shedding. The ADAM family proteins, which are highly expressed in some tumors, play a role in secreting growth factors, such as HB-EGF, and migration of cells. Thus, it is speculated that these proteins could be potential targets for tumor treatment (22). The present study is the first to show that clinically available anticancer drugs have an ability to modulate the expression of ADAM family proteins. They seem to suppress ADAM10 expression at a transcriptional level, but the precise mechanism of this suppression is not yet known.

The MICA ELISA system may not equally detect all soluble MICA (MICA molecules have >60 allelic variants). Our finding that soluble MICA could be detected in all HCC patients suggests that this system was applicable for our cohort of HCC patients. However, special caution should be paid for the use of this ELISA system for widely polymorphic MICA. Because CD44 is well known to be released into circulation from tumors by proteolytic cleavage of ADAM10 (23), the activity of ADAM10 in HCC tissues may be correlated with soluble CD44 levels. If so, our data suggest a close link between ADAM10 activity and the shedding of MICA in HCC. Furthermore, the decline in soluble MICA levels correlated well with the decline in soluble CD44 levels as early as 2 weeks after epirubicin-based TACE therapy. Reducing the tumor volume by such therapy may have led to both decreases but it is also possible that epirubicin suppresses ADAM10 activity, thereby inhibiting the shedding of MICA and CD44. Epirubicin may have a previously unrecognized role in cancer therapy; that is, affecting ADAM10 activity and MICA shedding rather than simply serving as a direct toxic agent for tumor cells.

Our data suggest that anti-HCC chemotherapy could remodel HCC cells, enhancing sensitivity to NK cells by upregulating MICA expression on the cellular surface. A concomitant decline in soluble MICA levels ameliorates NK cell ability by upregulating its NKG2D expression. We previously showed that activation of local innate antitumor immunity in liver tissues resulted in eliciting tumor-specific acquired immunity (21). If liver innate immunity is efficiently activated after anti-HCC chemotherapy, an additional antitumor effect against HCC cells could be expected. Immune modulators such as α-galactosylceramide have been shown to efficiently activate liver innate immune cells, including NK cells (21, 26). The combination therapy of anti-HCC chemotherapy and immunotherapy targeting NK cells might improve the antitumor effect of unresectable HCC and the prognosis of HCC patients.

In spite of recent progress in HCC therapies, there remains significant room for improvement, especially with respect to advanced liver cancer. We have shown here that anti-HCC chemotherapy resulted in enhanced NK sensitivity of HCC cells through inhibition of the activity of ADAM10 protease followed by modification of MICA expression. These findings indicate that efficient activation of liver innate immunity after anti-HCC chemotherapy might represent a particularly promising approach to suppress tumor growth and promote regression in liver cancer patients.

Disclosure of Potential Conflicts of Interest

No potential conflicts of interest were disclosed.

Acknowledgments

Received 3/4/09; revised 7/15/09; accepted 7/24/09; published OnlineFirst 10/13/09.

Grant support: Grant-in-Aid from the Ministry of Education, Culture, Sports, Science and Technology of Japan (T. Takehara) and Grant-in-Aid for Research on Hepatitis and BSE from the Ministry of Health, Labour and Welfare of Japan (N. Hayashi).

The costs of publication of this article were defrayed in part by the payment of page charges. This article must therefore be hereby marked *advertisement* in accordance with 18 U.S.C. Section 1734 solely to indicate this fact.

References

1. Fattovich G, Stroffolini T, Zagni I, Donato F. Hepatocellular carcinoma in cirrhosis: incidence and trends. Gastroenterology 2004;127:S35–50.
2. Bosch FX, Ribes J, Diaz M, Cleries R. Primary liver cancer: worldwide incidence and trends. Gastroenterology 2004;127:S5–16.
3. Takayasu K, Arii S, Ikai I, et al. Prospective cohort study of transarterial chemoembolization for unresectable hepatocellular carcinoma in 8510 patients. Gastroenterol 2006;131:461–9.
4. Doherty DG, O'Farrelly C. Innate and adaptive lymphoid cells in human liver. Immunol Rev 2000;174:5–20.
5. Mehal WZ, Azzaroli F, Crispe IN. Immunology of the healthy liver: old questions and new insights. Gatsroenterology 2001;120:250–60.
6. Bauer S, Groh V, Wu J, et al. Activation of NK cells and T cells by NKG2D, a receptor for stress-inducible MICA. Science 1999;285:727–9.
7. Groh V, Rhinehart R, Seceist H, Bauer S, Grabstein KH, Spies T. Broad tumor-associated expression and recognition by tumor-derived γδT cells of MICA and MICB. Proc Natl Acad Sci U S A 1999;96:6879–84.
8. Jinushi M, Takehara T, Tatsumi T, et al. Expression of MICA and MICB in human hepatocellular carcinomas and their regulation by retinoic acids. Int J Cancer 2003;104:354–61.
9. Wu JD, Higgins LM, Steinle A, Cosman D, Haugk K, Plymate SR. Prevalent expression of the immunostimulatory MHC class I chain-related molecule is counteracted by shedding in prostate cancer. J Clin Invest 2004;114:560–8.
10. Raffaghello L, Prigione I, Airoldi I, et al. Downregulation and/or release of NKG2D ligands as an immune evasion strategy of human neuroblastoma. Neoplasia 2004;6:558–68.
11. Ogasawara K, Lanier LL. NKG2D in NK and T cell-mediated immunity. J Clin Immunol 2005;25:534–40.
12. Coudert JD, Held W. The role of the NKG2D receptor for tumor immunity. Semin Cancer Biol 2006;16:333–43.
13. Groh V, Wu J, Yee C, Spies T. Tumor-derived soluble MIC ligands impair expression of NKG2D and T cell activation. Nature 2002;419:734–8.
14. Salih HR, Rammensee HG, Steinle A. Downregulation of MICA on human tumors by proteolytic shedding. J Immunol 2002;169:4098–102.
15. Salih HR, Antropius H, Gieseke F, et al. Functional expression and release of ligands for activating immunoreceptor NKG2D in leukemia. Blood 2003;102:1389–96.
16. Jinushi M, Takehara T, Tatsumi T, et al. Impairment of natural killer cell and dendritic cell functions by soluble form of MHC class I-related chain A in advanced human hepatocellular carcinoma. J Hepatol 2005;43:1013–20.
17. Kohga K, Takehara T, Tatsumi T, et al. Serum levels of soluble major histocompatibility complex (MHC) class I-related chain A in patients with chronic liver disease and changes during transcatheter arterial embolization for hepatocellular carcinoma. Cancer Sci 2008;99:1643–9.
18. Holdenrieder S, Stieber P, Peterfi A, Nagel D, Steinle A, Salih HR. Soluble MICA in malignant disease. Int J Cancer 2006;118:684–7.
19. Kaiser BK, Yim D, Chow IT, et al. Disulphide-isomerase-enabled shedding of tumor-associated NKG2D ligands. Nature 2007;447:482–6.
20. Waldhauer I, Goehlsdorf D, Gieseke F, et al. Tumor-associated MICA is shed by ADAM proteases. Cancer Res 2008;68:6368–76.
21. Tatsumi T, Takehara T, Yamaguchi S, et al. Intrahepatic delivery of α-galactosylceramide-pulsed dendritic cells suppresses liver tumor. Hepatology 2007;45:22–30.
22. Mochizuki S, Okada Y. ADAMs in cancer cell proliferation and progression. Cancer Sci 2007;98:161–7.
23. Anderegg U, Eichenberg T, Parthaune T, et al. Simon JC. ADAM10 is the constitutive functional sheddase of CD44 in human melanoma cells. J Invest Dermatol 2009;129:1471–82.
24. Nagano O, Murakami D, Hartmann D, et al. Cell-matrix interaction via CD44 is independently regulated by different metalloproteinases activated in response to extracellular domain Ca^{2+} influx and PKC activation. J Cell Biol 2004;165:893–902.
25. Boutet P, Aguera-Gonzalez S, Atkinson S, et al. The metalloproteinase ADAM17/TNF-α enzyme regulates proteolytic shedding of the MHC class I-related chain B protein. J Immunol 2009;182:49–53.
26. Miyagi T, Takehara T, Tatsumi T, et al. CD1d-mediated stimulation of natural killer T cells selectively activates hepatic natural killer cells to eliminate experimentally disseminated hepatoma cells in murine liver. Int J Cancer 2003;106:81–9.

Hepatology Research 2009; 39: 432–438 doi: 10.1111/j.1872-034X.2008.00477.x

Original Article

Effect of interferon α-2b plus ribavirin therapy on incidence of hepatocellular carcinoma in patients with chronic hepatitis

Mika Kurokawa,[1] Naoki Hiramatsu,[1] Tsugiko Oze,[1] Kiyoshi Mochizuki,[1] Takayuki Yakushijin,[1] Nao Kurashige,[1] Yuko Inoue,[1] Takumi Igura,[1] Kazuho Imanaka,[2] Akira Yamada,[3] Masahide Oshita,[4] Hideki Hagiwara,[5] Eiji Mita,[6] Toshifumi Ito,[7] Yoshiaki Inui,[8] Taizo Hijioka,[9] Harumasa Yoshihara,[10] Atsuo Inoue,[11] Yasuharu Imai,[12] Michio Kato,[6] Shinichi Kiso,[1] Tatsuya Kanto,[1] Tetsuo Takehara,[1] Akinori Kasahara[1] and Norio Hayashi[1]

[1]*Department of Gastroenterology and Hepatology, Osaka University Graduate School of Medicine,* [2]*Osaka Medical Center for Cancer and Cardiovascular Diseases,* [3]*Hyogo Prefectural Nishinomiya Hospital,* [4]*Osaka Police Hospital,* [5]*Higashiosaka City Central Hospital,* [6]*National Hospital Organization Osaka,* [7]*Kansai Rousai Hospital,* [8]*Hyogo Prefectural Nishinomiya Hospital,* [9]*National Hospital Organization Osaka Minami Medical Center,* [10]*Osaka Rousai Hospital,* [11]*Osaka General Medical Center and* [12]*Ikeda Municipal Hospital, Osaka, Japan*

Aim: The objective of this study was to elucidate the long-term effects of interferon (IFN)α-2b plus ribavirin combination therapy and to clarify whether this therapy can reduce the incidence of hepatocellular carcinoma (HCC) in patients with chronic hepatitis C.

Methods: A total of 403 patients infected with hepatitis C virus (HCV) were enrolled in a multicenter trial. All patients were treated with a combination of IFN-α-2b plus ribavirin therapy. We examined the incidence of HCC after combination therapy and analyzed the risk factors for liver carcinogenesis.

Results: A sustained virological response (SVR) was achieved by 139 (34%) of the patients. The cumulative rate of incidence of HCC was significantly lower in SVR patients than in non-SVR patients ($P = 0.03$), while there was no difference in the cumulative incidence of HCC between the transient response (TR) group and the no response (NR) group. Cox's regression analysis indicated the following risk factors as independently significant in relation to the development of HCC: age being > 60 years ($P = 0.006$), advanced histological staging ($P = 0.033$), non-SVR to IFN therapy ($P = 0.044$). The cumulative incidence rate of HCC was significantly lower in patients who had average serum alanine aminotransferase (ALT) levels of < 40 IU/L than in those who showed average serum ALT levels of ≧ 40 IU/L after the combination therapy ($P = 0.021$).

Conclusions: These results suggest that the attainment of SVR or continuous normalization of ALT levels after IFN therapy can affect patients apart from HCC development.

Key words: chronic hepatitis C, continuous normalization of ALT, hepatocellular carcinoma, interferon plus ribavirin combination therapy, sustained virological response

INTRODUCTION

HEPATOCELLULAR CARCINOMA (HCC) is one of the most common malignancies in Japan and its incidence has been increasing over the last 30 years. Recently, various treatments such as transcatheter arterial embolization/chemoembolization, radio frequency ablation and hepatic resection have been reported to yield significant improvements in overall patient survival,[1–3] but HCC relapse has thus far been observed in a majority of treated patients due to the highly malignant potential of the liver. In general, approximately 70–80% of Japanese HCC patients are also diagnosed with type C chronic hepatitis or cirrhosis.[4] It has also been shown that the chronic hepatitis C (CHC) liver slowly but steadily progresses to cirrhosis[5,6] and the risk of HCC increases according to the degree of liver fibrosis.[7,8] In this regard, the success of treatment

Correspondence: Dr Naoki Hiramatsu, Department of Gastroenterology and Hepatology, Osaka University Graduate School of Medicine, 2-2 Yamadaoka, Suita City, Osaka 565-0871, Japan. Email: hiramatsu@gh.med.osaka-u.ac.jp
Received 10 July 2008; revised 15 October 2008; accepted 2 November 2008.

for chronic hepatitis C virus (HCV) infection is expected to prevent the patient's liver from progressing to cirrhosis and to reduce the risk of development of HCC. Interferon (IFN) has been proven to be effective in reducing and in eliminating HCV from the circulation; in decreasing serum alanine aminotransferase (ALT) levels; and in improving the histological appearance of the liver in patients with CHC.[9–11] Moreover, it has been demonstrated that IFN monotherapy in CHC patients is associated with reducing the incidence of HCC, especially in those patients who achieved a sustained virological response (SVR).[12–14] Recently, many investigators have reported that combination therapy using IFN-α-2b or pegylated IFN (Peg-IFN) N plus ribavirin is more effective for eradicating HCV than IFN monotherapy.[15–17] However, it has not been accurately evaluated whether or not the combination therapy using Peg-IFN plus ribavirin could reduce HCC development in patients infected with HCV.

In this study, we evaluated the long-term effect of IFN-α-2b plus ribavirin therapy on the incidence of HCC in HCV-infected patients treated with the combination therapy by retrospective examination of the clinical outcomes.

METHODS

Patients

THIS STUDY WAS a multicenter trial conducted by Osaka University Hospital and other institutions participating in the Osaka Liver Forum in Japan. A total of 459 patients with HCV infection were treated with a combination of IFN-α-2b (Intron; Schering-Plough Corporation, Kenilworth, NJ, USA) plus ribavirin (Rebetol; Schering-Plough, Auxerre, France) between June 2002 and March 2005. All patients were treated with 6 MU of IFN-α-2b subcutaneously thrice a week and with oral ribavirin daily. Ribavirin was given at a total daily dose of 600 mg for patients who weighed < 60 kg and 800 mg for patients who weighed ≧ 60 kg. Patients who were positive for hepatitis B surface antigen, anti-human immunodeficiency virus antibody or those with other liver diseases (alcoholic liver disease, autoimmune liver disease, etc) were excluded from this study. Also excluded were patients with a history of HCC and those who developed HCC within the first 6 months of the follow-up period after the end of IFN therapy, because of the possibility that microscopic HCC had been present before initiation of the treatment. The remaining 403 patients infected with HCV were enrolled and followed in this study. The observation term was terminated upon the start of the next IFN therapy, such as Peg-IFN plus ribavirin after a combination of IFN-α-2b plus ribavirin therapy. Responses to IFN therapy were divided into the following three groups based on the viral load: sustained virological response (SVR) was defined as the absence of detectable serum HCV-RNA at 24 weeks after completion of IFN therapy. Transient response (TR) was defined as the absence of HCV-RNA from the serum at the end of treatment but detectable at 24 weeks after completion of therapy. Those categorized as having no response (NR) did not meet these criteria.

This study protocol followed the ethical guidelines of the 1975 Declaration of Helsinki, and informed consent was obtained from each patient.

Blood tests

Serum samples were stored frozen at −80°C. HCV-RNA levels were analyzed by quantitative reverse transcription (RT)–PCR assay (Amplicor-HCV version 2.0; Roche Diagnostic Systems, Tokyo, Japan). The lowest detection limit of this assay was 50 IU/mL. All patients were examined for serum HCV-RNA level and underwent hematological and biochemical tests just before therapy, every 4 weeks during treatment and every 12 weeks thereafter until the end of treatment.

Normal serum ALT is defined as < 40 IU/L. In addition, the biological response to IFN therapy was defined based on "the average serum ALT level", which was calculated from all data of ALT levels after completion of IFN therapy.

Histological evaluation

The patients underwent liver biopsies within 6 months before the start of therapy. Histopathological interpretation of specimens was done by experienced liver pathologists who had no clinical information. The histological appearance of the liver sample sections was evaluated according to METAVIR's histological score.[18] Fibrosis stage was evaluated on a scale from 0 to 4.

Diagnosis and follow up of HCC

Ultrasonography was carried out before IFN therapy and every 3 to 6 months during the follow-up period. New space-occupying lesions detected or suspected at the time of ultrasonography were further examined by computed tomography (CT) or hepatic angiography. HCC was diagnosed by the presence of typical hypervascular characteristics on angiography, in addition to the findings from CT. If no typical image of HCC was observed, fine-needle aspiration biopsy was carried out with the

patient's consent, or the patient was carefully followed until a diagnosis was possible with a definite observation by CT or angiography.

Statistical analysis

Quantitative variables were expressed as mean ± SD. The Kaplan–Meier method was used to calculate the cumulative incidence of HCC. The prognostic relevance of clinical variables and HCC incidence was evaluated by univariate analysis with log–rank test and by multivariate Cox's regression analysis. A value of $P < 0.05$ (two-tailed) was considered to indicate significance. All calculations were performed with SPSS version 15.0J (SPSS, Chicago, IL, USA).

RESULTS

Baseline characteristics in patients treated with interferon therapy

THE BASELINE CLINICAL features of the enrolled patients are shown in Table 1. The mean age of the patients was 55.8 ± 10.9 years, and 64% of the total cases were male. Two hundred and sixty-one patients (73%) were infected with HCV genotype 1 and had a viral load of more than 10^5 IU/ml. Liver biopsy was done for 320 cases and the ratio of patients with severe fibrosis (F3–4) diagnosed by the HAI score was more than 31%. The mean platelet count was 14.8 ± 5.1 × 10^4/μl, and the ALT level was 96.0 ± 62.6 IU/L. A sustained virological response (SVR) was achieved by 139 patients (34%) by combination therapy of IFN-α-2b plus ribavirin. According to an intent-to-treat analysis, 20% (51/261) of patients with HCV genotype 1 and a high viral load (≧ 100KIU/mL) achieved SVR by the combination therapy, whereas 75% (73/97) of the patients with HCV genotype 2 or a low load showed SVR. The median observation period for all patients was 36.5 ± 14.8 months with a range of 6 to 62 months from the end-point of IFN treatment.

Table 1 Baseline characteristics in patients treated with interferon therapy

	All cases
Number of patients	403
Age	55.8 ± 10.9
Gender (male/female)	257/145
Genotype and viral load (1H/non-1H)	261/97
Fibrosis (F0/1/2/3/4)	15/149/56/92/8
WBC (/μl)	5113 ± 1487
Platelet (× 10^4/μl)	14.8 ± 5.1
ALT (IU/l)	96.0 ± 62.6
IFN effect (SVR/TR/NR/cessation)	139/109/110/45

Data are number of patients, mean ± standard deviation. Fibrosis stage is evaluated on a scale from 0 to 4 according to METAVIR's histological score. 1H, Genotype 1 and high viral load; non-1H, all except for 1H; ALT, alanine aminotransferase; IFN, interferon; NR, no response; SVR, sustained virological response; TR, transient response; WBC, white blood cells.

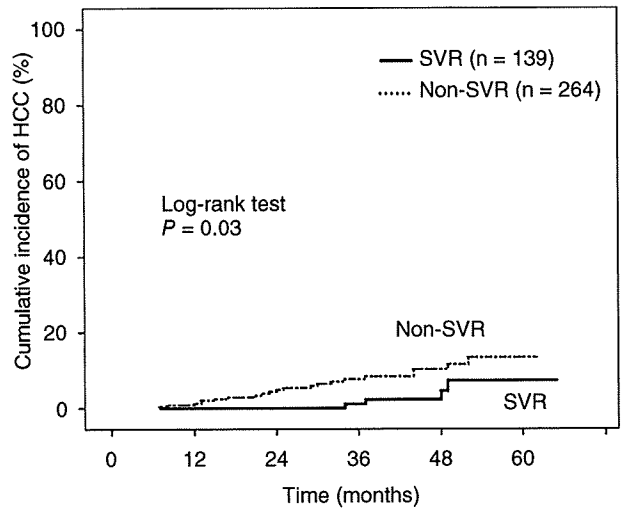

Figure 1 Cumulative incidence of development of hepatocellular carcinoma (HCC) according to treatment effect: (—) sustained virological response; (.....) non-sustained virological response.

Cumulative incidence of development of HCC according to the treatment effect (SVR vs. non-SVR)

Figure 1 shows the Kaplan–Meier estimates of the cumulative HCC incidence according to the treatment effect (SVR vs. non-SVR). Twenty-five (6%) of the 403 enrolled patients developed HCC; four (2.9%) of the SVR group and 21 (8.0%) of the non-SVR group. The cumulative incidence rate of HCC was significantly lower in patients of the SVR group than in those of the non-SVR group ($P = 0.03$).

Cumulative incidence of HCC development according to the treatment effect (SVR vs. TR vs. NR vs. cessation)

Figure 2 shows the Kaplan–Meier estimates of the cumulative HCC incidence according to the treatment effect (SVR vs. TR vs. NR vs. cessation). Five patients (4.6%) of the TR group, nine (8.2%) of the NR group and seven (15.6 %) of the cessation group developed